

INNATE IMMUNE MEMORY
AND PULMONARY EXPOSURE TO LIPOPOLYSACCHARIDES

EXAMINATION OF PHENOTYPIC AND FUNCTIONAL CHANGES
IN INNATE IMMUNE MEMORY
FOLLOWING LOCAL MUCOSAL EXPOSURE TO LIPOPOLYSACCHARIDE

By GLUKE YE, H.B.Sc.

A Thesis Submitted to the School of Graduate Studies in Partial Fulfillment of the
Requirements for the Degree Master of Science

McMaster University © Copyright by Gluke Ye, 2022

MASTER OF SCIENCE (2022)

McMaster University

(Medical Sciences)

Hamilton, Ontario

TITLE: Examination of Phenotypic and Functional
Changes in Innate Immune Memory Following
Local Mucosal Exposure to Lipopolysaccharide

AUTHOR: Gluke Ye, H.B.Sc (McMaster University)

SUPERVISOR: Dr. Zhou Xing

SUPERVISORY COMMITTEE: Dr. Ali Ashkar

Dr. Yonghong Wan

NUMBER OF PAGES: xiv, 70

Lay Abstract

The innate immune system is one of the first defenders in our bodies that fight against a variety of pathogens. In the last decade, the innate immune system was found to be capable of having memory, meaning it reacts faster or at a heightened magnitude in response to a wide range of subsequent pathogens after it is trained by an agent. This project explores the effect a bacteria wall component, LPS, has on the lung environment and examines if it will induce memory in the lung. Our findings show that intranasal exposure to LPS changes the cellular landscape in the lung. LPS-exposed airway innate immune cells become more activated and provide subsequent protection against bacterial infections. This work has implications for using LPS as a vaccine adjuvant in order to provide protection against a variety of pathogens in addition to specific protection brought by the vaccine.

Abstract

Innate immune memory has become an increasingly popular area of research in the last decade. However, much of the work done on innate immune memory using inflammatory agents such as BCG, *C. albicans*, and β -glucan has been pursued through systemic administration, which has been shown to induce training in circulating monocytes. In addition, little is known about whether microbial ligands can induce training. Here, we show that local mucosal exposure to an acute dose of LPS induces long-lasting phenotypic changes in airway macrophage populations. LPS-exposed macrophages display increased glycolytic metabolism and differential cytokine expression upon restimulation, whereas circulating monocytes are not affected. Finally, we show that LPS exposure provides long-lasting protection against *Streptococcus pneumoniae* in the lung, likely due to the higher acquisition of CD11b, which is indicative of macrophage activation and phagocytosis. As much of the work on innate immune memory has been done through systemic administration of training agents, this project aims to fill existing knowledge gaps in the induction of innate immune memory upon local mucosal exposure to inflammatory agents.

Acknowledgements

To my supervisor, Dr. Zhou Xing, thank you for your immense support and guidance over the past two years. You have given me the opportunity to gain unique learning experiences such as working in the CL3 facility, and the space to interact with the most intelligent people I have ever met on a regular basis. I have not just gained technical skills, but grown as a person and met lifelong friends thanks to you.

To my supervisory committee members, Dr. Ali Ashkar and Dr. Yonghong Wan, thank you for all your guidance and support throughout my training. I will never forget how mentally stimulating committee meetings were and I will surely miss them.

To all my current and past lab members, thank you for all your help, advice, and support throughout my training. It has been an honour to learn from all of you and I am so glad I got to experience my graduate program with you. Thank you, Kanwal, for your time and assistance on the glycolytic portion of my thesis, and many thanks to the staff at CAF, I could not have done this without you.

To my dearest friends Duffy and Jessie, and my family, Meiying, Jing, Kathy, Kayin, and Alex, thank you for your unwavering love and support throughout the past two years. You guys are the reason why I was able to accomplish this work.

Table of Contents

Lay Abstract.....	iv
Abstract	v
Acknowledgements	vi
Table of Contents	vii
List of Figures	xi
List of Abbreviations	xii
Declaration of Academic Achievement.....	xiv
1. INTRODUCTION	1
1.1 General Introduction.....	1
1.2 Concept of Trained Innate Immunity (TII).....	2
1.2.1 TII following systemic exposure to live organisms.....	3
1.2.2 TII following exposure to inflammatory agonists.....	5
1.2.3 TII following exposure to viruses	8
1.3 Pulmonary Resident Macrophages	9
1.3.1 Origin of Pulmonary Resident Macrophages.....	10
1.3.2 Pulmonary macrophages in host defense	11
1.3.3 Role of pulmonary macrophages in host defense against <i>Streptococcus pneumoniae</i>	12

1.4 Current knowledge and outstanding questions.....	14
1.5 Hypothesis.....	14
2. MATERIAL AND METHODS	15
2.1 Key Resources Table	15
2.2 Experimental Model.....	19
2.2.1 Mice	19
2.3 Method Details	19
2.3.1 Respiratory inoculation of lipopolysaccharide	19
2.3.2 Immunostaining and flow cytometry	20
2.3.3 In vivo labeling of resident alveolar macrophages.....	21
2.3.4 Purification of airway macrophages	22
2.3.5 Preparation of peripheral blood and bronchoalveolar lavage for ex vivo experiments	22
2.3.6 Metabolic assay of airway macrophages	22
2.3.7 Ex vivo secondary stimulation	23
2.3.8 Quantification of chemokines and cytokines	24
2.3.9 Respiratory infection by <i>Streptococcus pneumoniae</i>	24
2.3.10 Evaluation of clinical outcomes and bacterial infection in the lung and spleen	25

2.3.11 Statistical analysis.....	25
3. RESULTS	26
3.1 Objective 1: Characterize the phenotype of airway macrophage populations upon local mucosal exposure to LPS	26
3.1.1 Peak inflammation occurs 3 days post-LPS exposure	26
3.1.2 Kinetic changes of airway macrophage phenotype following local mucosal exposure to LPS	27
3.1.3 Bona fide AMs acquire CD11b expression following local mucosal exposure to LPS.....	28
3.2 Objective 2: Examine the functional outcomes of airway macrophage populations following local mucosal exposure to LPS	29
3.2.1 LPS induces heightened glycolytic capacity and reserve in airway macrophages 28 days post-LPS exposure	29
3.2.2 LPS-exposed airway macrophages respond differentially to <i>ex vivo</i> secondary stimulation	30
3.3.3 LPS exposure does not induce differential cytokine production in circulating monocytes following secondary stimulation	31
3.2.4 Responses of LPS-exposed mice to a secondary heterologous bacterial challenge <i>in vivo</i>	31

3.2.5 Local mucosal exposure to LPS induces faster CD11b acquisition in airway macrophages following sublethal infection of <i>S. pneumoniae</i>	32
4. DISCUSSION	50
5. CONCLUSIONS AND FUTURE DIRECTIONS	55
6. REFERENCES	58
7. SUPPLEMENTAL FIGURES	71

List of Figures

Figure 1	Illustration of the current understanding of trained innate immunity in the lung.	9
Figure 2	Peak inflammation occurs 3 days post-LPS exposure.	34
Figure 3	Kinetic changes in airway macrophage phenotype following local mucosal exposure to LPS.	36
Figure 4	Bona fide AMs acquire CD11b expression following local mucosal exposure to LPS.	38
Figure 5	LPS induces heightened glycolytic capacity and reserve in airway macrophages 14 days post-exposure.	40
Figure 6	LPS-exposed airway macrophages respond differentially to <i>ex vivo</i> secondary stimulation.	42
Figure 7	LPS exposure does not induce differential cytokine production in circulating monocytes following secondary stimulation.	44
Figure 8	Local mucosal exposure to LPS provides long-term protection against <i>S. pneumoniae</i> infections in the lung.	46
Figure 9	Local mucosal exposure to LPS induces faster CD11b acquisition in airway macrophages following sublethal infection of <i>S. pneumoniae</i> .	48
Figure 10	Illustration of main findings.	57
S1	Comprehensive flow cytometry gating strategy for airway macrophages in BAL.	71
S2	Comprehensive flow cytometry gating strategy for circulating monocytes in blood.	72

List of Abbreviations

Ad	Adenoviral-vectored vaccine
AM	Alveolar macrophage
AP-1	Activator protein 1
APC	Antigen presenting cell
BAL	Bronchoalveolar lavage
BCG	Bacille Calmette-Guerin
BMDM	Bone marrow-derived macrophage
<i>C. albicans</i>	<i>Candida albicans</i>
CFU	Colony-forming units
CR3	Complement receptor 3
DC	Dendritic cell
ECAR	Extracellular acidification rate
<i>E. coli</i>	<i>Escherichia coli</i>
FBS	Fetal bovine serum
IM	Interstitial macrophage
IRF	Interferon regulatory factors
LPS	Lipopolysaccharide
MARCO	Macrophage receptor with collagenous structure
MD-2	Myeloid differentiation factor 2
MDM	Monocyte-derived macrophage

<i>M. tuberculosis</i>	<i>Mycobacterium tuberculosis</i>
NF- κ B	Nuclear factor kappa B
NK	Natural killer
PAMP	Pathogen-associated molecular patterns
PBS	Phosphate-buffer solution
PGN	Peptidoglycan
PRR	Pattern recognition receptor
<i>S. aureus</i>	<i>Staphylococcus aureus</i>
<i>S. mansoni</i>	<i>Schistosoma mansoni</i>
<i>S. pneumoniae</i>	<i>Streptococcus pneumoniae</i>
TB	Tuberculosis
TII	Trained innate immunity
TLR	Toll-like receptor
TransAM	Transitioning AM
WCL	Whole-cell lysate
WT	Wild-type

Declaration of Academic Achievement

All research and experimentation in this thesis (Figures 1-10 and Appendices S1 – S2) were undertaken by Gluke Ye with contributions and assistance as follows. Animal handling and sacrifice was assisted by Ramandeep Singh (Figure 4). Flow cytometry was performed with the assistance of Dr. Sam Afkhami (Figure 4). Glycolytic assays were completed by Dr. Kanwaldeep Singh (Figure 5).

1. INTRODUCTION

1.1 General Introduction

For many years, it was thought that only the adaptive arm of immunity possesses memory. However, emerging research in the field has demonstrated that the innate immune system can have an altered response to a secondary challenge of the same or an unrelated antigen or microbe, a process now referred to as innate immune memory (Netea et al., 2016). This altered response can either be in the form of hyper-responsiveness, which is referred to as trained innate immunity (TII), or hypo-responsiveness, termed innate immune tolerance (Netea et al., 2016). Many innate cells were found to be capable of having innate immune memory, including but not limited to monocytes, tissue-resident macrophages, dendritic cells (DC), and natural killer (NK) cells (Netea et al., 2020). These innate cells can be trained by various live organisms, viruses, microbial ligands, and self-derived molecules (Netea et al., 2020). Our lab has previously shown that local exposure to adenoviral-vectored vaccines induces robust memory alveolar macrophages capable of protecting against heterologous infections in the lung, such as *Streptococcus pneumoniae* (*S. pneumoniae*), *Escherichia coli* (*E. coli*), and SARS-CoV-2 (Yao et al., 2018, Afkhami et al., 2022). Recent work in the lab has also shown that local exposure to β -glucan rendered treated mice higher survival rates after a lethal *S. pneumoniae* infection (unpublished data). To further explore the effects of local mucosal exposure to inflammatory agonists, this project will investigate whether local mucosal exposure to lipopolysaccharide (LPS) will

induce lasting changes in phenotypic and functional profiles of local and systemic cell populations. The findings from this study offer new knowledge in innate immune training in the respiratory mucosa and hold implications for developing of vaccine adjuvants and the therapeutic use of immunomodulatory agents against respiratory infections.

1.2 Concept of Trained Innate Immunity (TII)

Traditionally, immunological memory was thought to be an exclusive characteristic of the adaptive immune system, which is only present in vertebrates. Due to the growing knowledge of innate immunity, existing literature has indicated heightened responses to secondary infections induced by a primary encounter with a pathogen in plants as well as in non-vertebrates, which both lack an adaptive immune system (Hildemann et al., 1977, Hildemann et al., 1979, Sticher et al., 1997, Moret et al. 2003, Durrant et al., 2004, Pham et al., 2007, and Rodrigues et al., 2010). Over the years, observational studies and randomized controlled trials have suggested that Bacille Calmette-Guerin (BCG), the only licensed vaccine against tuberculosis (TB), can provide non-specific protection against unrelated pathogens (Netea et al., 2014, Uthayakumar et al., 2018). In the past few years, more studies have found cases of innate immune memory, defined as a “persisting re-set state of the innate immune system long after the initial antigen or microbial exposure, leading to altered responsiveness to the same or an unrelated antigen or microbe” (Netea et al., 2016, Gourbal et al., 2018, Xing et al., 2020,). Innate immune memory can either lead to hypo-responsiveness, known as “innate

immune tolerance”, or hyper-responsiveness, known as “trained innate immunity” (Netea et al., 2016, Xing et al., 2020). To this date, many innate cells have been found capable of having innate immune memory, including monocytes, tissue-resident macrophages, DCs, neutrophils, NK cells, innate lymphoid cells, and even stromal and epidermal stem cells (Netea et al., 2020).

Trained innate immune cells exhibit characteristics such as increased aerobic glycolysis, epigenetic modifications including H3K27ac and H3K4me3, as well as an increase in the production of proinflammatory cytokines (Netea et al., 2020). It has been found that all of the aforementioned pathways are interconnected with each other. For instance, the training agent may induce a shift from oxidative phosphorylation to aerobic glycolysis, of which substrates such as fumarate or acetyl-CoA from the citric acid cycle may act on downstream proteins involved in epigenetic reprogramming (Netea et al., 2020). These proteins, such as KDM5 histone demethylase and histone acetyltransferases, deposit chromatin marks, which change the DNA methylation and acetylation status and lead to the unfolding of the chromatin, making it more accessible for the transcription and expression of proinflammatory factors upon exposure to a secondary stimulus (Netea et al., 2020).

1.2.1 TII following systemic exposure to live organisms

Certain organisms have been shown to induce non-specific protection against heterologous infections. It has been known for decades that the BCG vaccine provides non-specific protective effects. In West African regions with high mortality

rates, BCG-vaccinated children had higher survival rates from infections other than tuberculosis (Garly et al., 2013). Similar results were seen in murine studies; BCG-vaccinated mice had higher survival rates against secondary infections with *Candida albicans* (*C. albicans*) and *Schistosoma mansoni* (*S. mansoni*) (van't Wout et al., 1992). This protection appeared to be partially mediated by T cell-independent mechanisms and involved activated tissue macrophages (Tribouley et al., 1978). Complementing this data are additional studies investigating the protection induced by *C. albicans*. When mice were inoculated with an attenuated strain of *C. albicans* that is avirulent and incapable of germinating, protection was seen against subsequent infections from a pathogenic strain of *C. albicans* and also *Staphylococcus aureus* (*S. aureus*) (Bistoni et al., 1986). This mechanism was proven to be independent of T cell responses when similar results were replicated in athymic mice (Bistoni et al., 1986). Additionally, this mechanism relies on macrophages and the production of pro-inflammatory cytokines such as CSF, TNF- α , IL-1, and IFN- γ (Bistoni et al., 1988, Vecchiarelli et al., 1989).

Recent work in animal models found that systemic administration of BCG trained circulating monocytes. Kaufmann and colleagues adoptively transferred bone marrow-derived macrophages (BMDMs) from BCG-trained mice into Rag1^{-/-} mice (Kaufmann et al., 2018). BMDMs from the BCG-treated mice exhibited differential epigenetic marks and transcriptional profiles (Kaufmann et al., 2018). Furthermore, BMDMs from BCG-treated mice protected the recipient mice from subsequent *Mycobacterium tuberculosis* (*M. tuberculosis*) infection (Kaufmann et

al., 2018). These results suggest that systemic inoculation of BCG can access the bone marrow, promote myeloopoiesis, and generate trained circulating monocytes with a unique epigenetic and transcriptomic signature. Most importantly, it explains how TII in myeloid cells can last for several months and sometimes up to a few decades (Riekmann et al., 2017).

1.2.2 TII following exposure to inflammatory agonists

Inflammatory agonists can also induce TII in animal models. In addition to BCG and *C. albicans*, initial work on innate immune memory used β -glucan as a systemic training agent and made several major discoveries on the underlying mechanisms of TII. β -glucan is composed of groups of β -D-glucose polysaccharides and is found in the cell walls of yeasts, bacteria, and fungi, such as *C. albicans* (Camilli et al., 2018). It acts as a pathogen-associated molecular pattern (PAMP) in many fungal infections and binds to Dectin-1, scavenger receptors, and complement receptor 3 (CR3) on host cells (Camilli et al., 2018). Of these receptors, Dectin-1 has been characterized with the most detail. The binding of β -glucan to Dectin-1 initiates a myriad of responses in macrophages, DCs, and neutrophils. This includes phagocytosis, oxidative burst, neutrophil degranulation, fungal killing, and the production of inflammatory lipid mediators, cytokines, and chemokines (Goodridge et al., 2009). Many key characteristics of TII, such as increased glycolysis, epigenetic rewiring, and increased cytokine responses upon secondary heterologous exposure, were defined by studying β -glucan in systemic models (Netea et al., 2020).

Another inflammatory agonist commonly used in innate immune memory is LPS, which is a major component of the outer membrane of gram-negative bacteria (Foster et al., 2007). LPS is comprised of the variable O antigen, core oligosaccharides, and Lipid A, which is a conserved component responsible for the toxicity of gram-negative bacteria (Murphy et al., 2017). LPS induces the dimerization of the toll-like receptor 4 (TLR4)-myeloid differentiation factor 2 (MD-2) complex upon binding (Murphy et al., 2017). During bacterial infections, LPS can detach from the membrane of gram-negative bacteria and is picked up by the host LPS-binding protein present in the blood or extracellular fluid in tissues, then transferred to CD14, an accessory protein for TLR4, which is present on the surface of macrophages, neutrophils, and dendritic cells (Murphy et al., 2017). Activation of TLR4 activates nuclear factor kappa B (NF- κ B), interferon regulatory factors (IRF), and activator protein 1 (AP-1), which are transcription factors that induce genes that code for type I interferons, inflammatory cytokines, chemokines, antimicrobial proteins and peptides, tissue-repair and coagulation factors, and metabolic regulators (Foster et al., 2007, Murphy et al., 2017). LPS has been known for its role in endotoxin tolerance, in which cells or organisms transiently become unresponsive to repeated or prolonged stimulation with a low dose of LPS. This type of immunosuppression is protective against certain forms of cytokine-induced inflammatory damage. For instance, studies have documented the neuroprotective effects of tolerance induced by both systemic and local administration of LPS to the cerebrum (Wendeln et al., 2018, Mizobuchi et al.,

2021). On the other hand, the training effects of LPS have only been examined in detail recently and remain somewhat controversial. It started over half a century ago when it was found that injection of mice with LPS conferred protection against *M. tuberculosis* 7-14 days later (Youmans et al., 1965). This was one of the first pieces of evidence of innate immune memory. Since then, pretreatment with LPS was found to reduce pathogen spread or increase survival after infection by *Cryptococcus neoformans*, *Salmonella enterica*, *S. aureus*, or group B *Streptococcus* (Seeley et al., 2016). Some argue that these models are still forms of LPS tolerance and that enhanced survival is rather mediated by LPS-induced epigenetic changes to genes that are resistant to tolerance, collectively referred to as non-tolerizable genes (Foster et al., 2007). Foster and colleagues have demonstrated that non-tolerizable genes include antimicrobial effector genes, which explains the protection seen in the aforementioned studies, and suggests that macrophages could be primed to become more responsive to subsequent activation signals (Foster et al., 2007).

With increasing research, many more microbial ligands that confer non-specific protection against lethal infections were identified. To illustrate, treatment with muramyl dipeptide, a peptidoglycan component, induced protection against *S. pneumoniae* and *Toxoplasma gondii* infections (Kalafati et al., 2020). Treatment with CpG oligodeoxynucleotide protected against subsequent experimental sepsis and *Escherichia coli* meningitis (Krahenbuhl et al., 1981). In addition, exposure to flagellin protected against *S. pneumoniae* and rotavirus (Munoz et al., 2010, Ribes

et al., 2014). These PAMPs activate pattern recognition receptors (PRRs), and downstream effects include epigenetic modifications, activation of signalling pathways that enhance antigen-presenting cell (APC) functions, and production of T cell-polarizing cytokines that shape the adaptive immunity to infection. This implies that stimulation with ligands or pathogens that express the same ligand can enhance responses upon subsequent exposure to an unrelated pathogen that also expresses ligands for the same PRR (Gardiner et al., 2016).

1.2.3 TII following exposure to viruses

Not only are live organisms, microbial ligands, and self-derived molecules able to exert non-specific protective effects against subsequent infections, but viruses also seem to have similar potential. In a study by Barton and colleagues, latent herpesvirus increased resistance to *Listeria monocytogenes* and *Yersinia pestis* in mice (Barton et al., 2007). Interestingly, local mucosal exposure to gammaherpesvirus depleted the entire resident alveolar macrophage pool, which is subsequently replenished by infiltrating circulating monocytes (Figure 1, Machiels et al., 2017). In our lab, adenoviral-vectored vaccines (Ad) were shown to induce TII as well. It was found that intranasal exposure to Ad results in long-lasting memory airway macrophages and strong TII against subsequent viral and bacterial respiratory infections in the lungs, such as SARS-CoV-2 and *S. pneumoniae* (Figure 1, Yao et al., 2018, D'Agostino et al., 2020, Afkhami et al., 2022). This process requires T cell help around five to seven days post-viral exposure. In contrast to gammaherpesvirus and perhaps due to the replication-

deficient nature of adenoviral-vectored vaccines, the AM pool is unaffected, and therefore memory AMs self-sustain independently of circulating monocytes and had upregulated expression of MHC II, defense genes, and increased glycolysis (Yao et al., 2016). Systemic exposure to Ad, on the other hand, does not train mucosal macrophages in the lungs (D'Agostino et al., 2020).

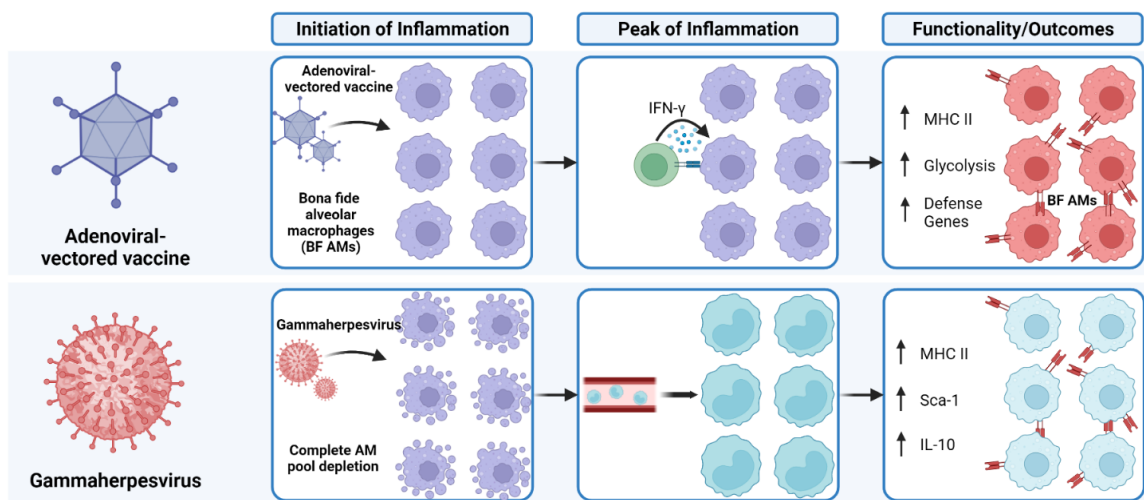


Figure 1. Current understanding of trained innate immunity in the lung.

Upon local mucosal exposure to adenoviral-vectored vaccines, the alveolar macrophage pool is retained and subsequently activated by T cells through contact-dependent interactions and IFN- γ production five to seven days later. This results in higher expression of MHC II, increased glycolysis, and increased expression of defense genes in AMs. In contrast, local mucosal exposure to gammaherpesvirus results in complete depletion of the AM pool. As a result, circulating monocyte are recruited to replace the AMs, and ultimately take on higher MHC II and Sca-1 receptor expression in addition to heightened IL-10 production.

1.3 Pulmonary Resident Macrophages

There are three subsets of macrophage populations in the lungs. One of the subsets includes alveolar macrophages (AMs), which are located in the alveoli and

are in close contact with type I and type II epithelial cells (Guilliams et al., 2013). The other two subsets of pulmonary resident macrophages are both interstitial macrophages (IMs), but the differences between these two subsets are less clear-cut (Guilliams & Svedberg 2021). Macrophages develop from different embryonic precursors such as the yolk sac, fetal liver, or bone marrow in overlapping stages from organogenesis to after birth (Guilliams & Svedberg, 2021). The exact contribution of distinct stages to the final pool of resident macrophages is highly debated, but most AMs likely develop from fetal liver monocytes, while the rest develop from bone marrow-derived monocytes and yolk-sac macrophages before birth (Guilliams & Svedberg, 2021). After birth, AMs populate the alveoli and self-renew under homeostatic conditions (Guilliams et al., 2013, Yona et al., 2013, Scott et al., 2014, Kopf et al., 2015, Van de Laar et al., 2016). In events of inflammatory insults, resident AMs may undergo varying extents of depletion, and bone marrow-derived monocytes are recruited to the lungs and believed to be shaped to become cells that closely resemble resident AMs by the local tissue microenvironment (Hashimoto et al., 2013, Lavin et al., 2014, Gibbings et al., 2015).

1.3.1 Origin of Pulmonary Resident Macrophages

It is still unknown to which extent circulating monocytes contribute to local defense during inflammation, as well as whether differences in macrophage ontogeny have any effect on their phenotype and functionality. However, one of the current beliefs proposed by Guilliams and Svedberg is that at steady state, the local microenvironment imprints a tissue-resident phenotype on macrophages and

restricts their plasticity regardless of ontogeny (Guilliams & Svedberg, 2021). This is thought to prevent unwarranted tissue damage and allow gas exchange. When the AM pool is significantly depleted to varying degrees during inflammation, monocytes are recruited to replenish the AM pool (Guilliams & Svedberg, 2021). They take on a stronger inflammatory signature than resident macrophages and are referred to as inflammation-imprinted resident macrophages (InfResMacs) (Guilliams & Svedberg, 2021). InfResMacs retain a portion of the inflammatory signature following the resolution of the inflammation, whereas resident macrophages return to their steady-state transcriptomic profile (Guilliams & Svedberg, 2021). As a result, any subsequent insult would induce a stronger reaction from InfResMacs compared to resident macrophages (Guilliams & Svedberg, 2021). As the inflammation resolves, a portion of recruited monocytes referred to as transient macrophages (TransMacs) die off and restore baseline macrophage numbers (Guilliams & Svedberg, 2021). After a prolonged absence of inflammation, InfResMacs eventually convert to resident macrophages and become restricted in their plasticity (Guilliams & Svedberg, 2021).

1.3.2 Pulmonary macrophages in host defense

During respiration, the upper and lower airways are constantly exposed to various airborne particles and microorganisms. As a result, there are elaborate systems in place to maintain homeostasis in the lung. AMs are a part of the frontline defense and are essential for the initiation and mediation of immune responses in the lung. Alveolar macrophages recognize antigens via surface receptors such as

TLRs and scavenger receptors like macrophage receptor with collagenous structure (MARCO) (Brooks et al., 2018). The binding of the antigen to these receptors initiates inflammatory pathways, such as the NF- κ B pathway, to upregulate the production of pro-inflammatory cytokines (Nelson et al., 2007). One of the other major roles of AMs is to phagocytose pathogens, which are then killed in low pH lysosomes (Hussell et al., 2014). Other immune cells such as neutrophils are recruited to the lungs if AMs fail to control the infection.

1.3.3 Role of pulmonary macrophages in host defense against Streptococcus pneumoniae

S. pneumoniae can cause severe diseases such as pneumonia, septicemia, and meningitis and is the leading cause of death by an infection in developed countries (Brooks et al., 2018). *S. pneumoniae* is a gram-positive, facultative anaerobic bacteria that is a part of the normal upper respiratory tract flora (Brooks et al., 2018). It does not pose significant risks under normal circumstances but can migrate to the lungs and become pathogenic when the host immune system is suppressed (Brooks et al., 2018). Once in the lungs, it can cause inflammation, which leads to air sacs filling with fluid, resulting in difficulty breathing for many patients (Brooks et al., 2018).

S. pneumoniae possesses a variety of proteins and toxins that drive its pathogenesis. The first wall of defense that *S. pneumoniae* encounters is the mucosa and respiratory epithelial cells. Goblet cells and ciliated respiratory cells function simultaneously to clear the pathogen in a process known as mucociliary

clearance (Nelson et al., 2007). Furthermore, respiratory epithelial cells can secrete cytokines and chemokines to recruit other cells and also produce antimicrobial peptides such as defensins, human apolactoferrin, and lysozymes (van der Poll et al., 2009). However, the bacteria contain many mechanisms to fight against antimicrobial peptides and evade being trapped by mucus. The next cells to encounter *S. pneumoniae* in the lung are AMs. Activation of AMs is dependent on PRRs, specifically TLR2, TLR4, and TLR9, in the context of *S. pneumoniae* infections (Dockrell et al., 2003). Macrophages attach to cells opsonized by the complement system and Fc γ receptors. Additionally, MARCO aids in phagocytosing non-opsonized antigens (Dockrell et al., 2003). AMs are capable of killing *S. pneumoniae* at low levels, but when overburdened, they secrete chemokines and cytokines to recruit neutrophils to the lung (Dockrell et al., 2003, Knapp et al., 2003). Neutrophils would subsequently fight against pneumococci with the release of extracellular traps and granules (Brooks et al., 2018).

Taut and colleagues demonstrated that in response to *S. pneumoniae* infections, rather than expanding pre-existing resident cells, populations of resident alveolar and lung parenchymal macrophages are replaced by infiltrating circulating monocytes (Taut et al., 2008). Given this fact and the importance of macrophages in host defense against *S. pneumoniae*, *S. pneumoniae* would make an ideal secondary stimulus to test whether systemic administration of β -glucan or Ad can train circulating monocytes to subsequently enhance local protection against bacterial infections in the lung.

1.4 Current knowledge and outstanding questions

The current understanding of TII is limited to systemic exposure to training agents, and the field has only recently begun to look at TII in local sites such as the brain, skin, and lungs. In the lung, nasally delivered adenoviral-vectored vaccines and gammaherpesvirus can induce long-lasting phenotypic changes and protection against subsequent insults (Figure 1, Yao et al., 2018, Machiels et al., 2018).

While we know that viruses and bacteria can induce training in pulmonary cell subsets, little is known about the administration of microbial agents to the lungs. LPS, especially, is ubiquitously present in the environment (Natarajan et al., 2010) and is frequently used to induce immune tolerance, but recent publications suggest that it is able to induce training as well, likely through epigenetic modifications on non-tolerizable genes which code for anti-microbial proteins (Gardiner et al., 2016). It remains unclear whether local mucosal exposure to LPS would induce training and if it will confer subsequent protection against respiratory bacterial infections such as ones induced by *S. pneumoniae*. Results would shed light on the aforementioned confusion surrounding LPS, explore innate immune memory in the context of the lung, and offer insight on the use of LPS as a potential immunomodulator or adjuvant in vaccines.

1.5 Hypothesis

We hypothesize that local mucosal exposure of BALB/c mice to an acute dose of LPS will induce innate immune memory in airway macrophages, which will

confer subsequent protection against heterologous infections. We aim to pursue the following objectives to test our hypothesis:

1. Characterize the phenotype of airway macrophage populations upon local mucosal exposure to LPS.
2. Examine the functional outcomes of airway macrophage populations following local mucosal exposure to LPS.

Our findings demonstrate the ability of an acute dose of LPS to induce innate immune memory and confer subsequent protection against secondary heterologous infections. It appears that LPS induces long-lasting phenotypic and functional changes in airway macrophages, characterized by an increase in CD11b expression of bona fide macrophages from the peak of inflammation, increased glycolytic capacity and reserve, differential cytokine expression upon secondary stimulation, and protection against bacterial infections.

2. MATERIAL AND METHODS

2.1 Key Resources Table

REAGENT or RESOURCE	SOURCE	IDENTIFIER
Antibodies		
Anti-mouse CD11b PE-Cy7 (Clone: M1/70)	BD Biosciences	Cat. No. 552850
Anti-mouse CD11c APC (Clone: HL3)	BD Biosciences	Cat. No. 550261
Anti-mouse CD16/CD32 Fc block (Clone: 2.4G2)	BD Biosciences	Cat. No. 553142

Anti-mouse CD24 BV650 (Clone: M1/69)	BD Biosciences	Cat. No. 563545
Anti-mouse CD3 V450 (Clone: 17A2)	BD Biosciences	Cat. No. 561389
Anti-mouse CD3 PerCP- Cy5.5 (Clone: 145-2C11)	BD Biosciences	Cat. No. 551163
Anti-mouse CD4 APC-Cy7 (Clone: GK1.5)	BD Biosciences	Cat. No. 552051
Anti-mouse CD8 PE (Clone: 53-6.7)	BD Biosciences	Cat. No. 553035

<i>Continued</i>		
REAGENT or RESOURCE	SOURCE	IDENTIFIER
Antibodies		
Anti-mouse CD8 FITC (Clone: 53-6.7)	BD Biosciences	Cat. No. 553031
Anti-mouse CD8 PE (Clone: 53-6.7)	BD Biosciences	Cat. No. 553032
Anti-mouse CD45 APC-Cy7 (Clone: 30-F11)	BD Biosciences	Cat. No. 557659
Anti-mouse CD45R V450 (Clone: RA3-6B2)	BD Biosciences	Cat. No. 560473
Anti-mouse CD64 PE (Clone: X54-5/7.1)	BioLegend	Cat. No. 139304
Anti-mouse IL-6 PE (Clone: MP5-20F3)	BioLegend	Cat. No. 504503
Anti-mouse Ly6C Biotin (Clone: HK1.4)	BioLegend	Cat. No. 128003
Anti-mouse Ly6G BV605 (Clone: 1A8)	BD Biosciences	Cat. No. 563005
Anti-mouse MHC II AF700 (Clone: M5/114.15.2)	Thermo Fisher Scientific	Cat. No. 56-5321-82
Anti-mouse Siglec-F PE- CF594 (Clone: E50-2440)	BD Biosciences	Cat. No. 562757
Anti-mouse TNF- α PerCP/Cyanine5.5 (Clone: MP6-XT22)	BioLegend	Cat. No. 506321
GolgiPlug Protein Transporter Inhibitor	BD Biosciences	Cat. No. 555029
Streptavidin Qdot800	Thermo Fisher Scientific	Cat. No. Q10173MP
REAGENT or RESOURCE	SOURCE	IDENTIFIER
Bacterial and Virus Strains		
<i>Streptococcus pneumoniae</i>	ATCC	ATCC Number: 6303
Recombinant human serotype 5 adenovirus expressing <i>M. tb</i> Antigen 85A (AdHu5Ag85A)	Dr. Zhou Xing McMaster University, Hamilton, ON, Canada	
Biological Samples		
2-Mercaptoethanol	ThermoFisher Scientific	Cat. No. 21985023
BSA	Sigma-Aldrich	Cat. No. 10735086001
Cytofix/Cytoperm	BD Biosciences	Cat. No. 554714
Defibrinated sheep blood	Hemostat	Cat. No. DSB100

<i>Continued</i>		
REAGENT or RESOURCE	SOURCE	IDENTIFIER
Biological Samples		
FBS	ThermoFisher Scientific	Cat. No. 16140071
HEPES	ThermoFisher Scientific	Cat. No. 15630080
L-Glutamine	ThermoFisher	Cat. No. A2916801
Lipopolysaccharide from <i>E. coli</i> O55:B5	Sigma-Aldrich	Cat. No. L2880
MEM Non-Essential Amino Acids Solution	ThermoFisher Scientific	Cat. No. 11140076
Neomycin sulfate	Sigma-Aldrich	CAS Number: 1405-10-3
Penicillin-Streptomycin	ThermoFisher	Cat. No. 15140122
Peptidoglycan from <i>Staphylococcus aureus</i>	Sigma-Aldrich	Cat. No. 77140
PharmaLyse	BD Biosciences	Cat. No. 555899
Seahorse XF DMEM medium	Agilent Technologies	Cat. No. 103575-100
Sodium Pyruvate	ThermoFisher Scientific	Cat. No. 11360070
Todd Hewitt broth	BD Biosciences	Cat. No. 249240
Tryptic soy agar	BD Biosciences	Cat. No. 236950
Tryptic soy broth	BD Biosciences	Cat. No. 211825
Turk blood diluting fluid	RICCA Chemical	Cat. No. 8850-16
Whole cell lysate from Bacille Calmette-Guerin	Bei Resources	Cat. No. NR-14822
Critical Commercial Assays		
Aqua dead cell staining kit	ThermoFisher Scientific	Cat. No. L34957
DuoSet ELISA	R&D Systems	Cat. No. DY210-05
MILLIPLEX MAP Mouse Cytokine/Chemokine Magnetic Bead Panel	Millipore Sigma	Cat. No. MCYTOMAG-70K
Seahorse XF Glycolytic Stress Test Kit	Agilent Technologies	Cat. No. 103020-100
Experimental Models: Organisms/Strains		
Mouse: BALB/cJ	The Jackson Laboratory	IMSR Cat. No. JAX:000651
IDENTIFIER		
Mouse: BALB/c	Charles River	IMSR Cat. No. CRL:547

<i>Continued</i>		
REAGENT or RESOURCE	SOURCE	IDENTIFIER
Software and Algorithms		
FlowJo, version 11	https://www.flowjo.com	RRID: SCR_008520
GraphPad Prism, version 8	https://www.graphpad.com/scientific-software/prism/	RRID: SCR_002798
Wave Desktop, version 2	Agilent Technologies	https://www.agilent.com/en/products/cell-analysis/software-download-for-wave-desktop
xPONENT	ThermoFisher Scientific	https://www.luminexcorp.com/xponent
Other		
CD3 ϵ Microbead Kit, mouse	Miltenyi Biotec	Cat. No. 130-094-973
Cell Culture Microplate	Agilent Technologies	Cat. No. 101085-004
PKH26 Dye	Sigma-Aldrich	Cat. No. PKH26PCL-1KT

2.2 Experimental Model

2.2.1 Mice

Female wild-type BALB/c mice aged six-to-eight-week-old were purchased from Jackson Laboratory. All mice were kept in a specific pathogen-free level B facility at the McMaster Animal Facilities. Experiments were conducted in accordance with the guidelines from the Animal Research and Ethics Boards.

2.3 Method Details

2.3.1 Respiratory inoculation of lipopolysaccharide

Six-to-eight-week-old female BALB/c mice were intranasally (i.n.) inoculated with either 15 μ g of LPS (Sigma-Aldrich) in a single 25 μ L bolus of sterile phosphate-

buffered saline (PBS), or received PBS-only controls. Body weight, and clinical signs or illness were monitored following LPS exposure.

2.3.2 Immunostaining and flow cytometry

The number of mononuclear cells from bronchoalveolar lavage (BAL) were quantified and then plated in U-bottom 96 flat-bottom well-plates in a total volume of 200 μ L of culture media (RPMI 1740 with 2% fetal bovine serum (FBS), 1% L-glutamine, 1% penicillin/streptomycin). The cells were subsequently washed twice with PBS, then stained with the Aqua dead cell staining kit (ThermoFisher Scientific) for 30 minutes in the dark and at room temperature. After washing with PBS and then 0.5% BSA-PBS, cells were incubated with Fc block (ThermoFisher) in 0.5% BSA-PBS for 15 minutes on ice. Cells were finally stained with extracellular fluorochrome-labeled monoclonal antibodies for 30 minutes on ice.

For intracellular staining, 150 μ L of blood was diluted 1:2 in RPMI 1640 and immediately restimulated with either 50ng/mL of LPS (Sigma-Aldrich) or 1.6 μ g/mL of whole cell lysate (WCL) of BCG (BEI Resources). Three hours post-incubation, 50 μ L of GolgiPlug (BD Biosciences) diluted 1:100 in RPMI 1640 was added to each sample and incubated for 12 hours in a 37°C, 5% CO₂ incubator. Following incubation, 20mM of EDTA was added to each tube to achieve a final concentration of 100 μ L/mL. Tubes were then vortexed at high speed and incubated at room temperature for 10 minutes. Subsequently, 2mL of 1x PharmaLyse (BD Biosciences) diluted in distilled water was added to each sample, which was then

vortexed and incubated at room temperature for 15 minutes. At the end of incubation, cells were spun and resuspended in Aqua dead cell staining kit (ThermoFisher Scientific) at room temperature and in the dark for 30 minutes. Cells were then washed, and 100 μ L of Cytfix/Cytoperm (BD Biosciences) was added to samples for 20 minutes of incubation. After another wash, cells were blocked with Fc block in 0.5% BSA-PBS for 15 minutes on ice and then stained with fluorochrome-labeled monoclonal antibodies for 30 minutes on ice.

For intracellular staining of BAL samples, airway macrophages were incubated with ice-cold 0.5% BSA-PBS for 15 minutes twice, followed by minimal scraping to remove remaining adhering cells. Cells were then subjected to staining by the Aqua dead cell staining kit (ThermoFisher Scientific) in the dark at room temperature for 30 minutes. Following incubation, the cells were washed and subjected to permeabilization and fixation by Cytfix/Cytoperm (BD Biosciences) for 20 minutes. After another wash, cells were blocked with Fc block in 0.5% BSA-PBS for 15 minutes on ice and then stained with fluorochrome-labeled monoclonal antibodies for 30 minutes on ice.

2.3.3 In vivo labeling of resident alveolar macrophages

Mice were inoculated with 20 μ M of PKH26 dye (Sigma-Aldrich) in 50 μ L Diluent B (Sigma-Aldrich) 48 hours before LPS administration. BAL was collected 3 and 14 days after LPS exposure for cellular phenotyping by flow cytometry.

2.3.4 Purification of airway macrophages

Single-cell suspensions of BAL were labeled with CD3 ϵ microbeads (Miltenyi Biotec) to exclude T cells. Purified airway macrophages were used for *ex vivo* culture experiments, including metabolic assays, secondary stimulation, and cytokine and chemokine experiments.

2.3.5 Preparation of peripheral blood and bronchoalveolar lavage for ex vivo experiments

All mice were euthanized by exsanguination. Peripheral blood and BAL were collected. Peripheral blood was resuspended in RPMI for flow cytometry intracellular staining. Isolated cells from BAL were resuspended in cRPMI medium (RPMI 1740 with 2% FBS, 1% L-glutamine, 1% penicillin/streptomycin, and 10mM HEPES) for *ex vivo* experiments or in PBS for flow cytometry staining.

2.3.6 Metabolic assay of airway macrophages

Real-time cell metabolism of airway macrophages was assessed using the Seahorse Glycolysis Stress Test Kit (Agilent Technologies). Airway macrophages were purified from BAL by excluding T cells using CD3 ϵ microbeads (Miltenyi Biotec) and plated onto a 96-well microplate (Agilent Technologies) at a density of 7.5×10^4 cells/well, in a total volume of 100 μ L of enriched cRPMI media (RPMI 1740 supplemented with 10% FBS, 1% L-glutamine, 1% penicillin/streptomycin, 10mM HEPES, 0.5mM sodium pyruvate, 0.1mM non-essential amino acids, and 55 μ M 2-

mercaptoethanol) to avoid cell adhesion to the side of wells. The cells were left at room temperature for one hour before adding another 100 μ L of enriched cRPMI to all wells and subsequently incubated in a 37°C 5% CO₂ incubator for one hour. Following cell adhesion, cells were washed twice with warm PBS to remove the remaining non-adhering cells. Airway macrophages were then incubated overnight in enriched cRPMI media in a 37°C 5% CO₂ cell culture incubator. The next day, airway macrophages were washed twice with Seahorse XF DMEM medium with 2mM L-glutamine (Agilent Technologies) and resuspended in 180 μ L of the same media. Extracellular Acidification Rates (ECAR) were measured using a Seahorse XFe96 Analyzer (Agilent Technologies). Glycolysis and glycolytic capacity were represented as the ECAR after the addition of glucose and oligomycin, respectively. Glycolytic reserve was calculated by the difference between glycolytic capacity and glycolysis. All data were subsequently normalized to protein concentrations derived from the Bradford assay and analyzed using the Wave Desktop software (Agilent Technologies).

2.3.7 Ex vivo secondary stimulation

Isolated alveolar macrophages were resuspended in AM media (RPMI 1740 supplemented with 2% FBS, 1% L-glutamine, 1% penicillin/streptomycin, and 1x HEPES) and plated at 10⁵ cells/well in a 96 flat-bottom well-plate (200 μ L/well). Cells were incubated in a 37°C 5% CO₂ cell-culture incubator for two hours and were subsequently stimulated with either 50ng/mL of LPS (Sigma-Aldrich) or

1.6 μ g/mL of whole cell lysate (WCL) of BCG (BEI Resources). Following 12 hours of stimulation, supernatants were collected for cytokine and chemokine analysis.

For intracellular staining, 50 μ L of GolgiPlug diluted 1:100 in either RPMI or AM media for blood and BAL, respectively, was added to samples three hours following the addition of secondary stimulants (e.g., PGN, LPS, WCL). After 10 hours of stimulation, cells were prepared for intracellular staining as outlined in 2.3.2.

2.3.8 Quantification of chemokines and cytokines

Chemokines including IL-1 β , TNF- α , IL-6, KC, MCP-1, MIP-1 α , IP-10, and MIP-2 were quantified by using the (Millipore) kit according to the manufacturer's instructions. Plates were read using the xPONENT (ThermoFisher Scientific) software on a MagPix reader (ThermoFisher Scientific).

The proinflammatory cytokine TNF- α was quantified using the DuoSet ELISA kit (R&D Systems). ELISA plates were read at 450nm on a spectrophotometer.

2.3.9 Respiratory infection by *Streptococcus pneumoniae*

A clinical isolate of *Streptococcus pneumoniae* (*S. pneumoniae*) serotype 3 (ATCC 6303) was used to induce a sublethal bacterial infection in LPS-exposed mice. Frozen bacterial stock was plated on tryptic agar (BD Biosciences) supplemented with 5% defibrinated sheep blood (Hemostat) and 10 μ g/ml neomycin (Sigma-Aldrich) and incubated for six hours. Muroid colonies were subsequently cultured in Todd Hewitt broth (BD Biosciences) at 37°C in 5% CO₂

to mid-logarithmic phage ($OD_{600}=0.40$). Bacteria were then harvested and resuspended in PBS and kept on ice until infection. The dose was confirmed ten hours after plating 10-fold serial dilutions on blood agar plates. BALB/c mice were intratracheally (i.t.) inoculated with 10^5 colony-forming units (CFU) of *S. pneumoniae* in $40\mu\text{L}$ of PBS either 14 or 28 days post-LPS exposure.

2.3.10 Evaluation of clinical outcomes and bacterial infection in the lung and spleen

Mice were monitored daily for illness scores and weight changes following sublethal bacterial infection. All mice were sacrificed either six or twelve hours post-infection for further analysis by flow cytometry, or bacterial CFU assay and chemokine/cytokine analysis, respectively. To assess bacterial burden, lungs and spleen tissues were homogenized in ice-cold PBS supplemented with 10% glycerol and 0.1% Tween80. 10-fold serial dilutions were subsequently plated on blood agar plates and incubated overnight at 37°C in 5% CO_2 . Colonies were quantified ten hours later and calculated as CFU per organ.

2.3.11 Statistical analysis

The number of mice per group and statistical significance are reported in the figures and figure legends. A p-value of < 0.05 was considered significant (* $p < 0.05$, ** $p < 0.01$, *** $p < 0.001$, **** $p < 0.0001$). Two-tailed student t-tests were

used to compare groups. All analyses were performed by using GraphPad Prism software (Version 8).

3. RESULTS

3.1 Objective 1: Characterize the phenotype of airway macrophage populations upon local mucosal exposure to LPS

3.1.1 Peak inflammation occurs 3 days post-LPS exposure

Current literature points to the importance of dose on the type of training induced by LPS. Since extremely low doses of LPS are known to induce training, we attempted to follow doses typically used in acute lung injury models. To verify whether the dose can induce acute lung injury in BALB/c mice, we intranasally administered 15 μ g of LPS in a single 25 μ L bolus of sterile PBS to six-to-eight-week-old female BALB/c mice (Figure 2A). In agreement with the peak inflammation observed in ALI models using this dose, animals that received LPS transiently lost weight (9%) for two days prior to recovering on day 3 (Figure 2B). Elevated levels of MIP-1 α , KC, and MIP-2 were observed in BAL 3 days following LPS exposure (Figure 2C). Concurrently, increased infiltration of neutrophils and thus total cell count in the airways were also observed at this time point (Figures 2E and 2F). The above results indicate that the dose used in this model is able to induce acute lung injury, as it is consistent with findings in the literature.

3.1.2 *Kinetic changes of airway macrophage phenotype following local mucosal exposure to LPS*

To further examine airway macrophage populations collected from BAL, we next conducted cellular profiling to differentiate between monocyte-derived macrophages (MDMs; Ly6C^{hi}SiglecF⁻CD11b^{hi}), interstitial macrophages (IMs; Ly6C⁻SiglecF⁻CD11b^{hi}), and alveolar macrophages (AMs; Ly6C⁻SiglecF^{hi}CD11b⁻) using a comprehensive gating strategy previously described by Yao et al. 2018 (Figure S1). In contrast to PBS-inoculated control mice, LPS treatment was associated with a transient increase in MDMs on day 3, which returned to baseline levels by day 14 (Figures 3B and 3F). IMs were readily detectable by three days post-LPS administration, remaining detectable up to day 28 (Figures 3C and 3F). In contrast to the MDM and IM subpopulations, BF AMs were transiently depleted by day 3, returning to baseline levels by day 14. Interestingly, another airway macrophage population was identified on day three and subsequently named “transitioning alveolar macrophages” (TransAMs; Ly6C⁻SiglecF^{hi}CD11b⁺). Unlike AMs, these TransAMs expressed high levels of CD11b. The number of TransAMs readily increased up to day 21-post LPS administration (Figures 3E and 3F).

We then further assessed CD11b expression on individual populations since it indicates activation status in macrophages. IMs express high levels of CD11b at the peak of inflammation (day 3) as expected and subsequently declines until day 28 (Figure 3G). TransAMs follow the same trend, although surprisingly at levels that are two-fold higher than those of IMs (Figure 3G). It is also interesting to note

that TransAMs expressed lower levels of SiglecF compared to BF AMs (Figure 3F) and BF AMs also lost SiglecF expression until day 14 (Figure 3G).

These results indicate the emergence of phenotypically different populations in the airways. Importantly, BF AM counts decreased at peak inflammation following local mucosal exposure to LPS. It became a pressing matter to address whether BF AMs acquired CD11b expression to make up the TransAM population that appeared on day three or if TransAMs were myeloid-derived macrophages that transitioned into resident AMs.

3.1.3 Bona fide AMs acquire CD11b expression following local mucosal exposure to LPS.

To address the origin of the TransAM population, PKH26 dye was administered intratracheally 48 hours before LPS exposure to label BF AMs (Figure 4A). BAL was collected for airway cellular profiling on days three and 14. On day three, the majority of IMs were PKH-negative (Figures 4B and 4C), indicative of monocytic origin in these populations. Interestingly, a portion of BF AMs was also PKH-negative, which suggests that monocytes were recruited to replenish the pool of BF AMs (Figures 4B and 4C). These changes persisted up to day 14, although at a lower magnitude than those of day three.

Remarkably, TransAMs and some IMs on day three were PKH-positive, which suggests the ability of BF AMs to acquire CD11b and lose SiglecF expression after LPS exposure (Figures 4B, 4C, and 4D). On day 14, the BF AM population became

largely PKH-positive again, concurrent with an increase in absolute numbers of BF AMs (Figures 4B and 3D). This implies the transition of BF AMs back to the baseline phenotype profile as inflammation resolves.

It is important to note that BF AMs also acquired low levels of CD11b after PKH administration (Figures 4B and 4C), which confirms the association of CD11b to the activation status of macrophages, potentially linked to phagocytosis of the dye. All of the above data suggest the ability of BF AMs to gain CD11b and lose SiglecF expression at the peak of inflammation, as well as replenishment of the AM pool by circulating monocytes, which die off during the resolution of inflammation.

3.2 Objective 2: Examine the functional outcomes of airway macrophage populations following local mucosal exposure to LPS

3.2.1 LPS induces heightened glycolytic capacity and reserve in airway macrophages 28 days post-LPS exposure

Increased glycolysis is a characteristic of training observed in many TII studies. To examine metabolism, airway macrophages were collected on days 14 and 28 and rested overnight prior to performing glycolytic stress test (Figure 5A). Mice that received intranasal adenoviral-vectored vaccine (Ad) 6 weeks prior were used as a positive control (Yao et al. 2018). Ad showed increased glycolysis, glycolytic capacity, and glycolytic reserve at both time points (Figures 5B and 5C). There were no significant differences in glycolysis, glycolytic capacity, and glycolytic reserve between untreated and LPS-treated groups at day 14 (Figures 5B – 5E). However, glycolytic capacity and glycolytic reserve were significantly higher in the

LPS-treated group on day 28. It seems that it takes time for changes in metabolism to take place. Nevertheless, LPS induces changes in metabolism that are seen long after a single LPS exposure.

3.2.2 LPS-exposed airway macrophages respond differentially to ex vivo secondary stimulation

Another key characteristic of TII is heightened cytokine production upon secondary stimulation, namely heightened TNF- α and IL-6 production in a number of *ex vivo* β -glucan training models. Thus, the following experiment was done to determine whether LPS-exposed airway macrophages will produce heightened recall responses following both *ex vivo* homologous and heterologous stimulation. On day 14, airway macrophages were collected, rested, then subjected to secondary stimulation by LPS or WCL from BCG (Figure 6A). There were relatively low levels of most chemokines in both the naïve and LPS group at rest (Figure 6B). Upon restimulation with LPS, the LPS group produced significantly lower TNF- α , IP-10, and MCP-1 but higher KC and MIP-1 α (Figure 6B). Following heterologous stimulation with WCL, there were no differences in most chemokines between both groups other than increased KC (Figure 6B). This points to the superior ability of LPS-exposed airway macrophages to recruit and activate neutrophils. To conclude, LPS-exposed airway macrophages exhibit differential cytokine production *ex vivo* in response to LPS restimulation or WCL stimulation.

3.3.3 LPS exposure does not induce differential cytokine production in circulating monocytes following secondary stimulation

Since local mucosal exposure to bacterial ligands, such as β -glucan, is able to induce systemic training (unpublished data), we assessed the effect of LPS exposure on circulating monocytes. Briefly, blood was collected 14 days after LPS exposure and rested for an hour prior to secondary restimulation by LPS, stimulation by peptidoglycan (PGN), or by WCL (Figure 7A). Three hours later, GolgiPlug was added, and samples were analyzed by flow cytometry after ten hours of stimulation (Figure 7A). There were no significant differences in the percentage of both Ly6C^{hi} and Ly6C^{lo} monocytes that produced TNF- α and IL-6 (Figure 7B). The above data suggest that LPS-induced differences in cytokine production are limited to the lung.

3.2.4 Responses of LPS-exposed mice to a secondary heterologous bacterial challenge in vivo

Next, we sought to address whether different airway cell subsets and cytokine responses induced by LPS could provide protection against heterologous microbial challenges *in vivo*. On days 14 and day 28, mice were subjected to a sublethal dose (10^5 CFU) of *S. pneumoniae* intratracheally and sacrificed 12 hours later for bacterial burden in the lung and spleen (Figure 8A). Naïve mice lost around 2% of their original weight, whereas mice treated with LPS 28 days before the challenge maintained their weight 12 hours post-infection (Figure 8B). There were similar

amounts of CFU in the naïve group at both time points (Figure 8C). In the LPS group, there was around a log reduction in the LPS group compared to the naïve group 14 days post-LPS exposure and a little over half a log reduction 28 days post-LPS exposure (Figure 8C). To conclude, these results demonstrate the ability of local mucosal exposure to LPS to confer protection against *S. pneumoniae* *in vivo* up to 28 days following exposure.

3.2.5 Local mucosal exposure to LPS induces faster CD11b acquisition in airway macrophages following sublethal infection of S. pneumoniae

Next, we examined the potential mechanism for enhanced protection against heterologous bacterial infection in LPS-exposed lungs through cellular profiling following infection. Similar to the previous experiment, mice were infected with 10^5 CFU of *S. pneumoniae* intratracheally (Figure 9A). This time, BAL was collected six hours post-infection for cytokine or chemokine analysis and also cellular profiling (Figure 9A). LPS-treated mice had significantly more cells in the BAL before *S. pneumoniae* challenge and seemed higher following infection ($p=0.0525$, Figure 9B). This is largely in part due to a significant number of neutrophils being recruited to the airways in both groups, with numbers being slightly higher in the LPS group (Figures 9C and 9D). The number of IMs was higher in the LPS group both before and after the challenge, although it seemed to drop slightly in the LPS group post-infection (Figure 9E), indicating death due to *S. pneumoniae*. There were no differences in the number of BF AMs before infection, which is consistent with results from previous experiments (Figures 9F and 3D). Interestingly, the

number of BF AMs decreased in both groups following infection, although less in LPS ($p=0.10$), and TransAM numbers increased in both groups following infection (Figures 9F – 9H). This increase would likely be due to BF AMs acquiring CD11b expression in both groups, with LPS-exposed BF AMs acquiring CD11b expression faster. The above results suggest that activation, indicated by CD11b expression, likely hints at a higher inflammatory state and possibly higher phagocytic activity. Likewise, LPS exposure lowered lung bacterial burden due to having higher numbers of CD11b⁺ cells (i.e., IMs and TransAMs) present in the airways. There were no significant differences in cytokine or chemokine production between the two groups other than TNF- α production post-infection (Figure 9I). This is consistent with previous *ex vivo* data and suggests that LPS may have suppressed TNF- α to limit excessive inflammation. The lack of weight loss in the LPS group supports this hypothesis.

Figure 2

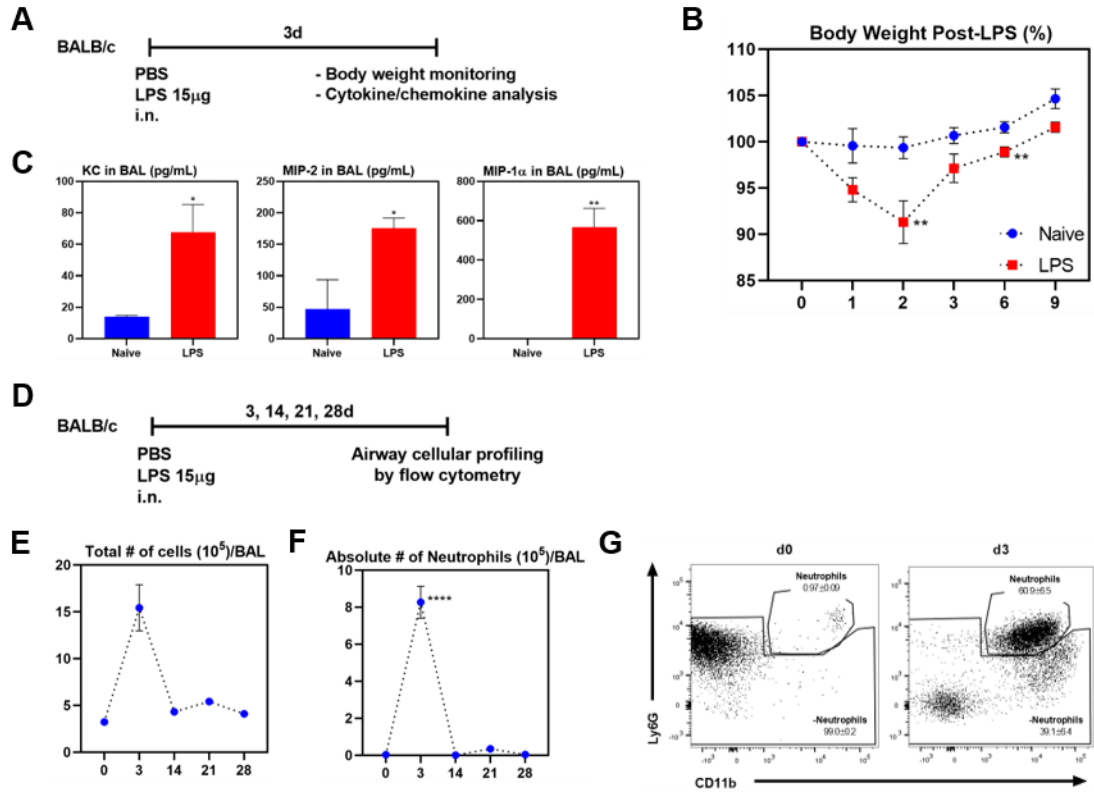


Figure 2. Peak inflammation occurs 3 days post-LPS exposure.

- (A) Experimental schema.
- (B) Percentage of body weight loss post-LPS exposure.
- (C) Cytokine and chemokine levels in conventional BAL 3 days post-LPS exposure.
- (D) Experimental schema.
- (E) Total number of cells in BAL upon LPS exposure.
- (F) Absolute number of neutrophils in BAL upon LPS exposure.
- (G) Flow plots of the neutrophil gate 3 days post-LPS exposure.

Data in (B) are pooled from four independent experiments (n=3 mice/group/time point). Data in (C) and (G) are from one experiment (n=3 mice/group). Data in (E) and (F) are representative of four independent experiments (n=3 mice/group/time point). Data in (B), (C), (E) – (G) represent mean \pm SEM. Statistical analysis for (B), (C), (E), and (F) were two-tailed t tests. *p < 0.05; ** p < 0.01; *** p < 0.001; ****p < 0.0001.

Figure 3

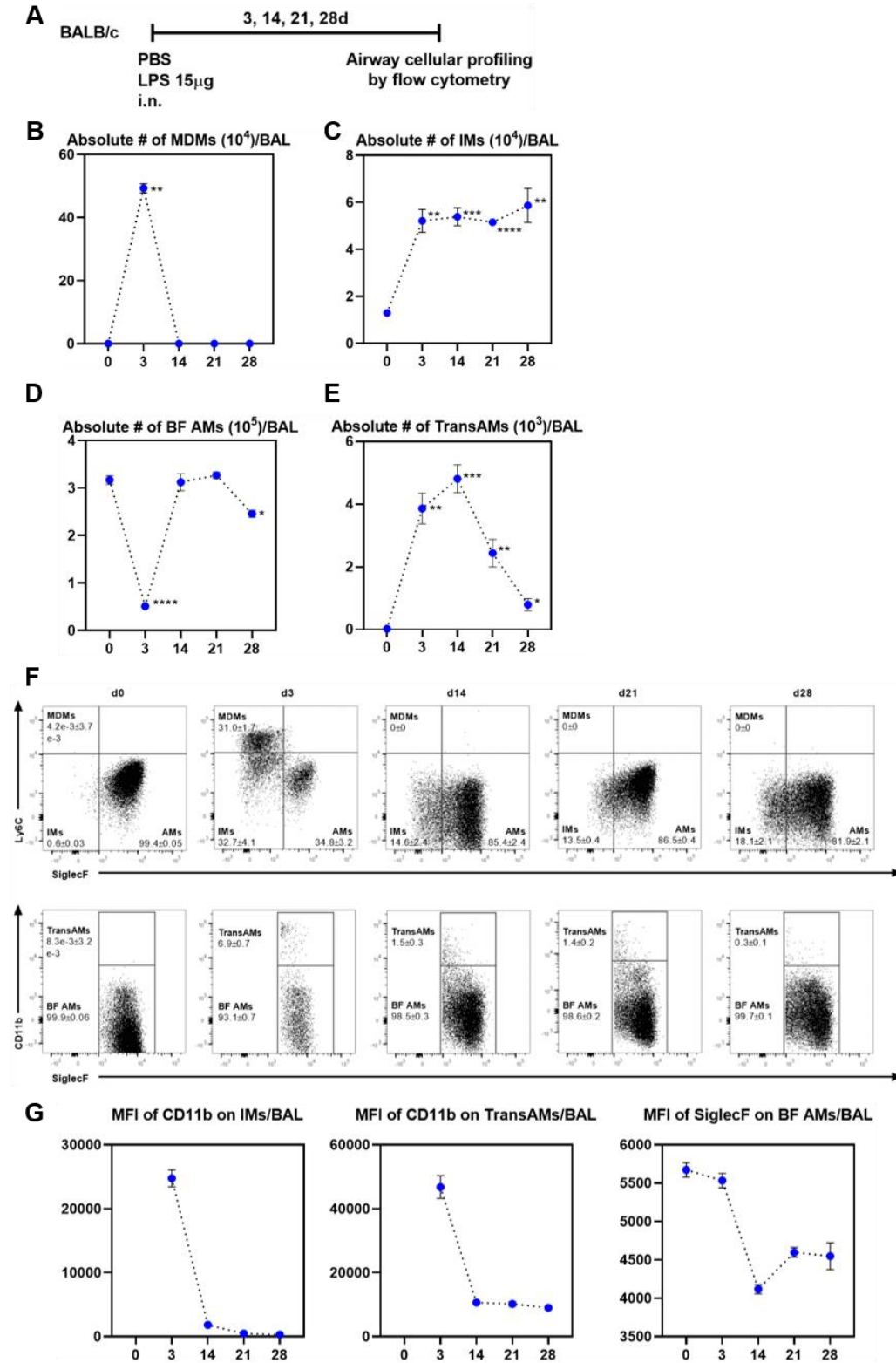


Figure 3. Kinetic changes in airway macrophage phenotype following local mucosal exposure to LPS

- (A) Experimental schema.
- (B) Absolute number of monocyte-derived macrophages (MDMs) in BAL upon LPS exposure.
- (C) Absolute number of interstitial macrophages (IMs) in BAL upon LPS exposure.
- (D) Absolute number of bona fide (BF) alveolar macrophages (AMs) in BAL upon LPS exposure.
- (E) Absolute number of transitioning alveolar macrophages (TransAMs) in BAL upon LPS exposure.
- (F) Flow plots of the terminal gates in BAL upon LPS exposure.
- (G) MFI of CD11b and SiglecF in airway macrophages.

Data in (B) – (G) are representative of four independent experiments (n=3 mice/group/time point). Data in (B) – (G) represent mean \pm SEM. Statistical analysis for (B) – (E) and (G) were two-tailed t tests. *p < 0.05; ** p < 0.01; *** p < 0.001; ****p < 0.0001.

Figure 4

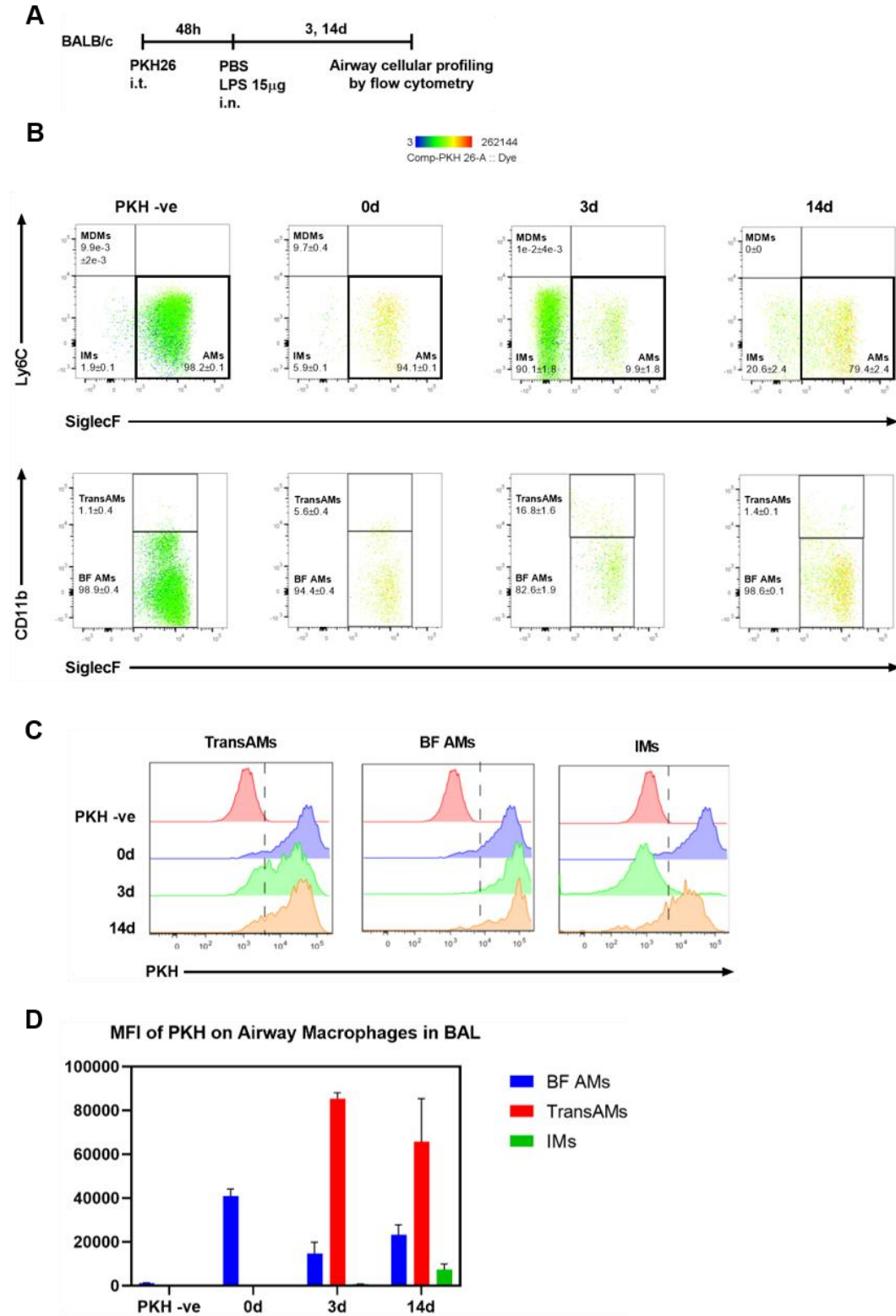


Figure 4. Bona fide AMs acquire CD11b expression following local mucosal exposure to LPS.

- (A) Experimental schema.
- (B) Flow plots of the terminal gates on day 0, 3, and 14 days post-LPS exposure. Colours represent varying degrees of PKH expression.
- (C) Histograms of airway macrophage populations at different time points.
- (D) MFI of PKH on different airway macrophage subsets.

Data in (B) – (D) are representative of two independent experiments (n=3 mice/group/time point). Data in (B) and (D) represent mean \pm SEM. Statistical analysis for (B) and (D) were two-tailed t tests. *p < 0.05; ** p < 0.01; *** p < 0.001; ****p < 0.0001.

Figure 5

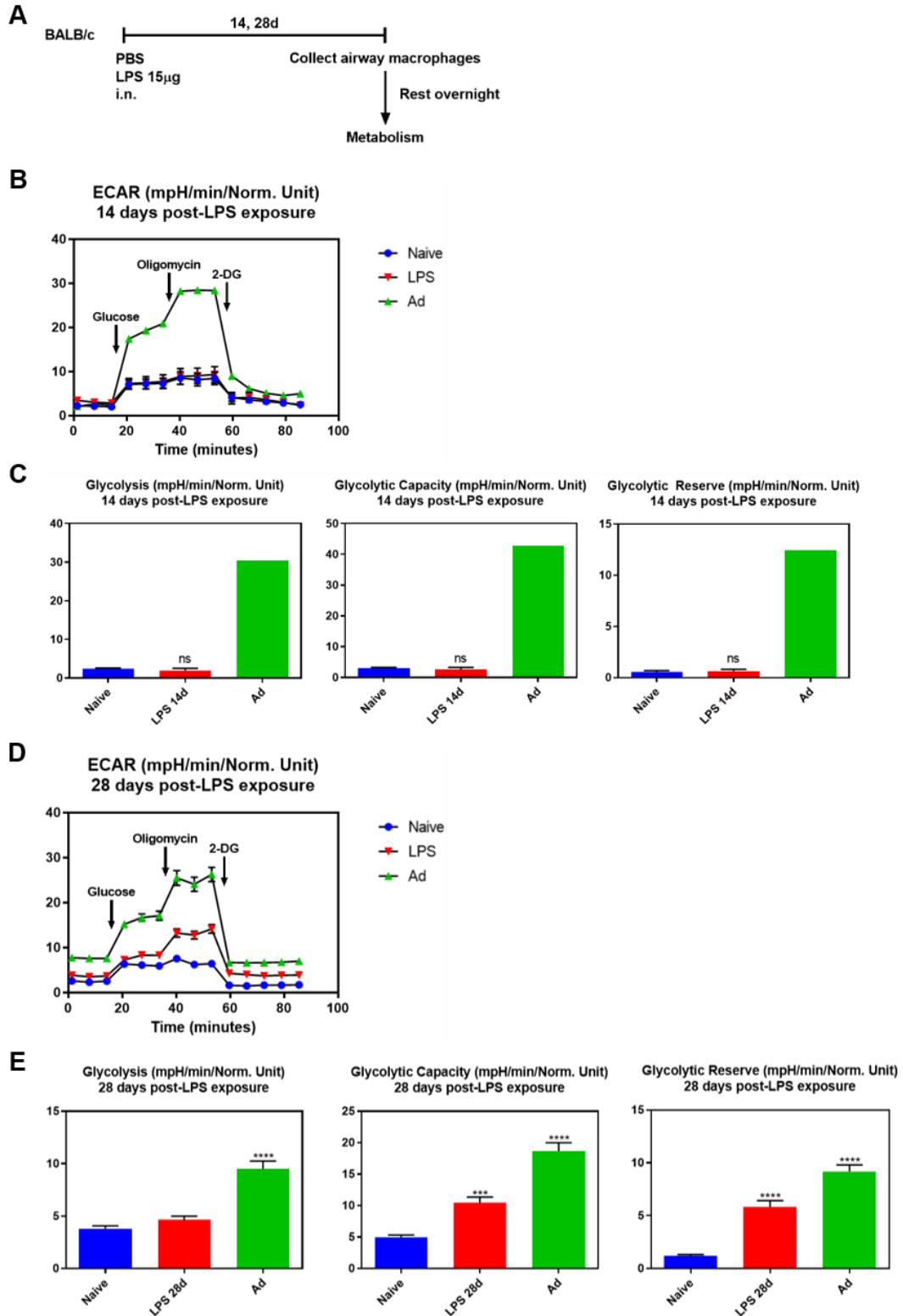


Figure 5. LPS induces heightened glycolytic capacity and reserve in airway macrophages 14 days post-exposure.

- (A) Experimental schema.
- (B) Real-time extracellular acidification rate (ECAR) in airway macrophages 14 days post-LPS exposure.
- (C) Glycolysis, glycolytic capacity, and glycolytic reserve in airway macrophages 14 days post-LPS exposure.
- (D) Real-time extracellular acidification rate (ECAR) in airway macrophages 28 days post-LPS exposure.
- (E) Glycolysis, glycolytic capacity, and glycolytic reserve in airway macrophages 28 days post-LPS exposure.

Data presented in (B) and (C) are from one experiment (n=3 mice pooled into 6 samples/group/time point). Data presented in (D) and (E) are from one experiment (n=3 mice pooled into 6 samples/group). Data in (B) – (E) represent mean \pm SEM. Statistical analysis for C and E were two-tailed t tests. *p < 0.05; ** p < 0.01; *** p < 0.001; ****p < 0.0001.

Figure 6

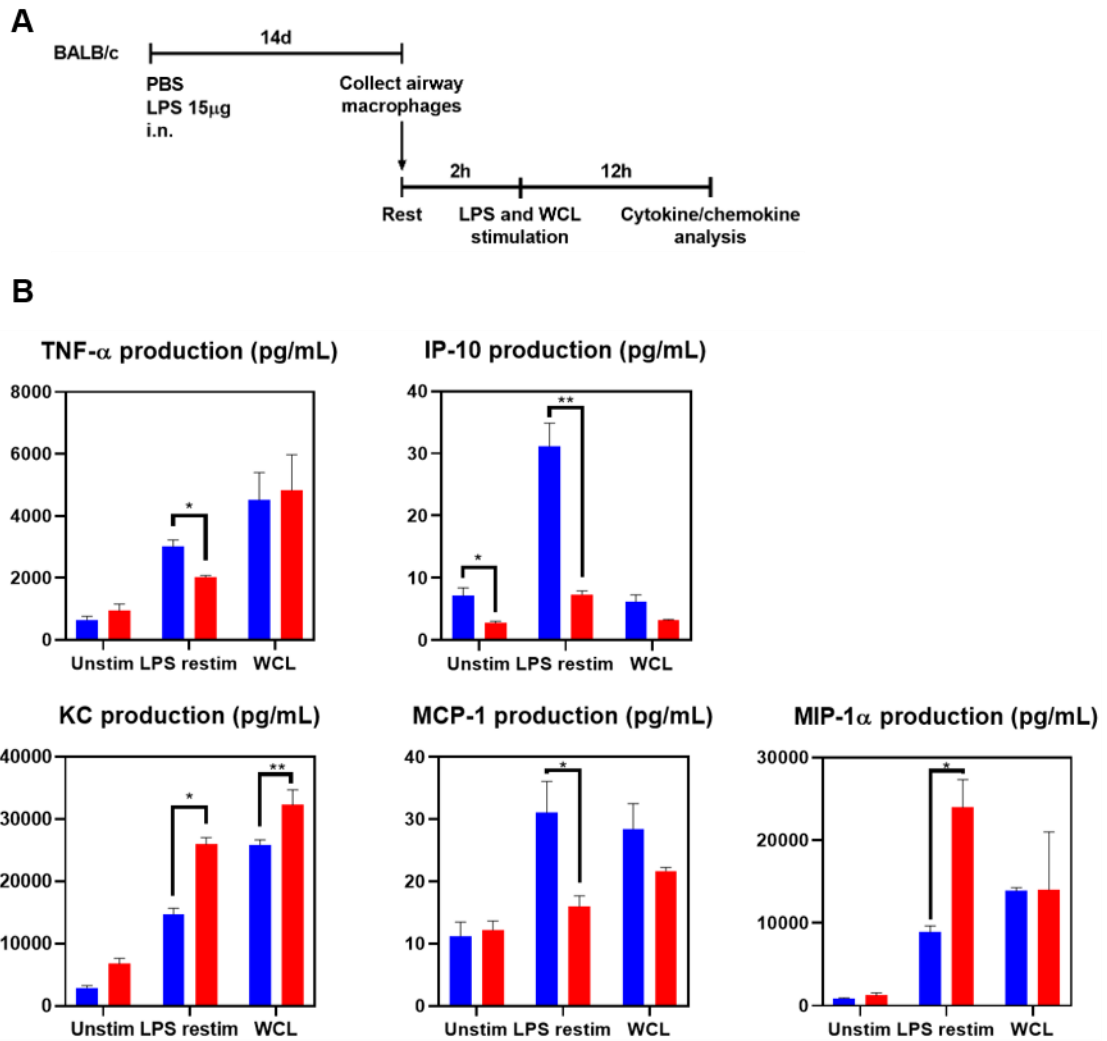


Figure 6. LPS-exposed airway macrophages respond differentially to *ex vivo* secondary stimulation.

(A) Experimental schema.

(B) Levels of TNF- α , IP-10, KC, MCP-1, and MIP-1 α produced following secondary stimulation *ex vivo*.

Data in (B) is from one experiment (n=3 mice/group). Data in (B) represent mean \pm SEM. Statistical analysis for (B) were two-tailed t tests. *p < 0.05; ** p < 0.01; *** p < 0.001; ****p < 0.0001.

Figure 7

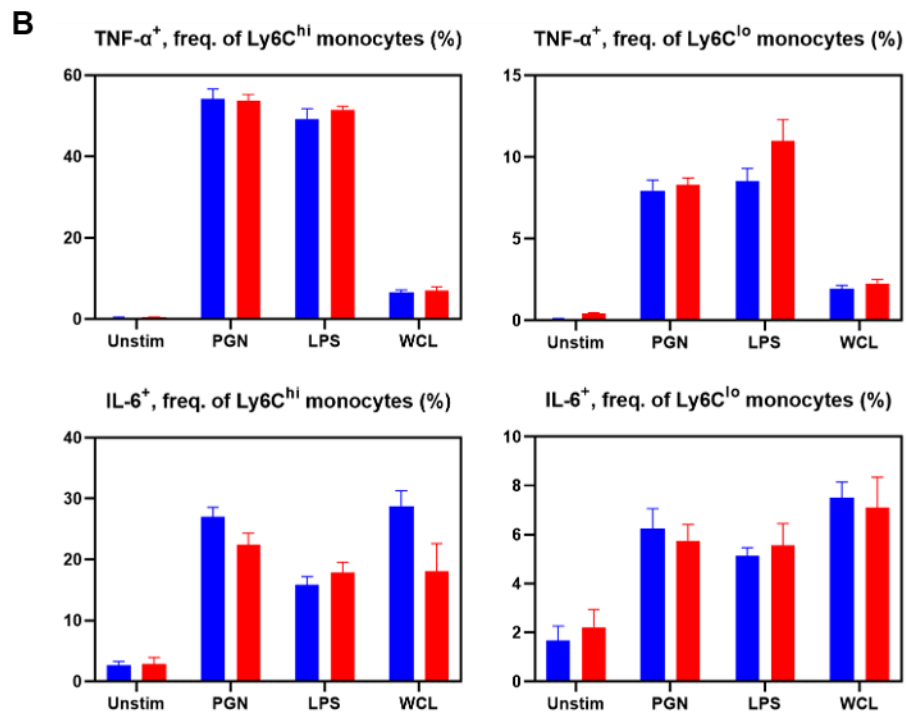
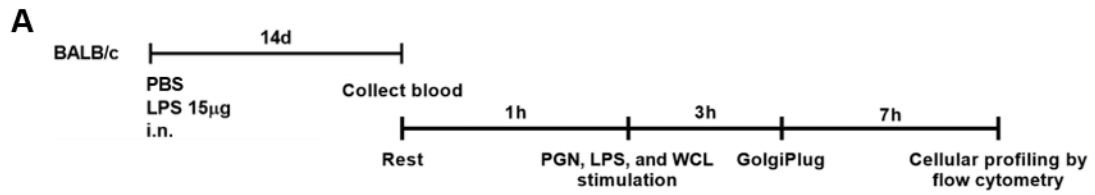


Figure 7. LPS exposure does not induce differential cytokine production in circulating monocytes following secondary stimulation.

(A) Experimental schema.

(B) Percentage of Ly6C^{hi} and Ly6C^{lo} monocytes producing TNF- α or IL-6.

Data presented in (B) are from one experiment (n=3 mice/group). Data in (B) represent mean \pm SEM. Statistical analysis for (B) were two-tailed t tests. *p < 0.05; ** p < 0.01; *** p < 0.001; ****p < 0.0001.

Figure 8

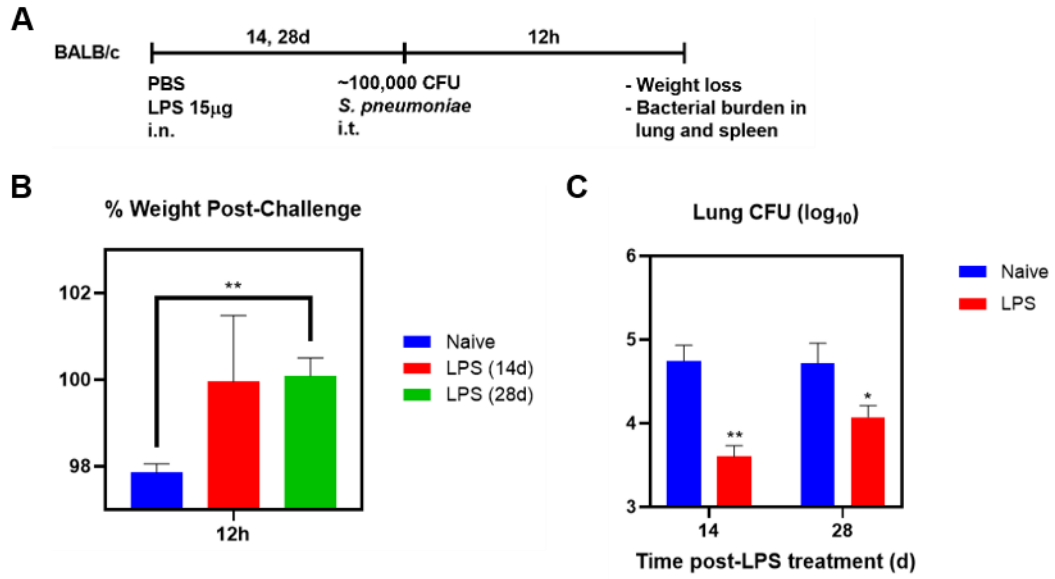


Figure 8. Local mucosal exposure to LPS provides long-term protection against *S. pneumoniae* infections in the lung

- (A) Experimental schema.
- (B) Percentage of weight loss 12 hours post-infection.
- (C) Bacterial CFU in the lung 12 hours post-infection.

Data in (B) and (C) are representative of two independent experiments (n=5 mice/group/time point). Data in (B) and (C) represent mean \pm SEM. Statistical analysis for (B) and (C) were two-tailed t tests. *p < 0.05; ** p < 0.01; *** p < 0.001; ****p < 0.0001.

Figure 9

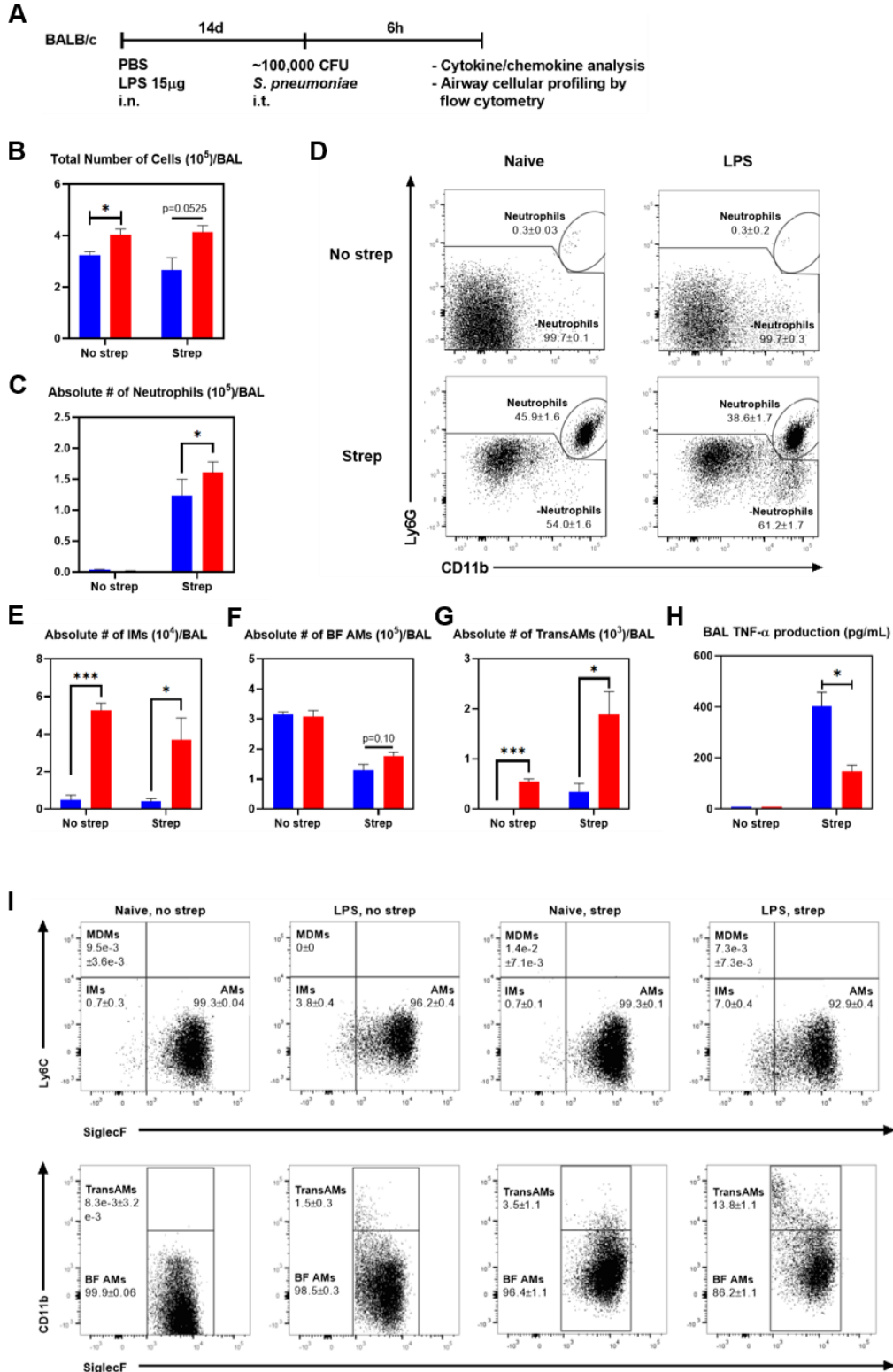


Figure 9. Local mucosal exposure to LPS induces faster CD11b acquisition in airway macrophages following sublethal infection of *S. pneumoniae*

- (A) Experimental schema.
- (B) Total number of cells in BAL post-infection.
- (C) Absolute number of neutrophils in BAL post-infection.
- (D) Flow plots of the neutrophil gate post-infection.
- (E) Absolute number of IMs in BAL post-infection.
- (F) Absolute number of BF AMs in BAL post-infection.
- (G) Absolute number of TransAMs in BAL post-infection.
- (H) Levels of TNF- α produced in the BAL following secondary heterologous challenge to *S. pneumoniae*.
- (I) Flow plots of the terminal gates post-infection.

Data in (B) – (I) are from one experiment (n=3 mice/group). Data in (B) – (I) represent mean \pm SEM. Statistical analysis for (B), (C), and (E) – (H) were two-tailed t tests. n=3 mice/group. *p < 0.05; ** p < 0.01; *** p < 0.001; ****p < 0.0001

4. DISCUSSION

This project demonstrates the ability of local mucosal exposure to LPS to induce phenotypic and functional changes long after the initial exposure. This dose, which closely follows doses used in LPS-induced ALI models, induced peak inflammation on day 3, which is marked by large numbers of infiltrating neutrophils (Figures 2F and 2G), an increase in neutrophilic chemokines (Figure 2C), and significant depletion of the AM pool (Figure 3D), likely due to pyroptosis facilitated by Caspase-1 (Wu et al., 2015). To replenish the airway macrophage pool, there was also infiltration of MDMs and IMs on day 3 (Figures 3B, 3C, and 3F), which are both SiglecF⁻ and CD11b⁺. Interestingly, a portion of alveolar macrophages expressed high CD11b at day 3 (Figures 3F and 3G), even more so than IMs and MDMs, and was consequently coined TransAMs. Yin and colleagues found that CD11b expression in AMs indicates an inflamed status, marked by elevated secretion of inflammatory cytokines and enhanced phagocytic capacity in the context of ALI (Yin et al., 2020). Consistent with this, the administration of the dye PKH26 induced acquisition of CD11b by BF AMs in LPS-exposed hosts (Figure 4B), pointing to the likely association between phagocytosis or activation with CD11b acquisition. Since phagocytosis by airway macrophages is thought to be essential in the resolution phase to phagocytose pathogens and apoptotic neutrophils (Cheng et al., 2020), the acquisition of CD11b is likely associated with recovery as well as protection against subsequent bacterial infections.

There were no significant differences in glycolysis between groups on day 14 and 28 (Figures 5C). Since an acute dose of LPS was given, it is likely that the system returned to rest by day 14 and was no longer in acute need of rapid energy production as seen during inflammation or intermediate products to be diverted to biosynthetic pathways (Riksen & Netea, 2021). Higher glycolytic capacity and glycolytic reserve was observed in airway macrophages on day 28, but not on day 14 (Figures 5C and 5E). This shows that LPS-exposed airway macrophages are better at switching from oxidative phosphorylation to using glycolysis in the event of inflammation induced by a secondary pathogen. It also indicates a higher theoretical glycolysis maximum in airway macrophages that were exposed to LPS, which is also beneficial upon secondary stimulation.

Local mucosal exposure to LPS induced differential cytokine production upon LPS restimulation or WCL stimulation compared to naïve airway macrophages (Figure 6B). In addition, the responses to WCL and LPS were not always comparable. This could be due to the nature of WCL, which contains a mixed bag of mycobacterial antigens, or it can be due to the fact that a training agent will not induce the same type of responses to different secondary stimulation since their downstream effects differ. Accordingly, local mucosal exposure to LPS did not provide protection in BALB/c mice following infection with a mouse-adapted strain of SARS-CoV-2 (unpublished data). LPS exposure did not have any effects on the cytokines and chemokines produced by circulating monocytes (Figure 7B), likely due to the low dose of LPS being given, which resulted in control within the lungs.

That being said, the possibility of LPS providing systemic protection cannot be fully eliminated, and additional experiments should be carried out to examine local mucosal effects of LPS on the circulation.

Local mucosal exposure to LPS resulted in a lower bacterial burden in the lungs on both days 14 and 28, although slightly lower at the later time point (Figure 8C). It is likely that the effects of LPS wane as time passes. As hypothesized by Guilliams and Svedberg, InfResMacs, the equivalent of TransAMs in this project, become restricted in their plasticity over time and converts to a phenotype akin to BF AMs throughout the resolution of inflammation. This restricted plasticity likely restricts the cells in the magnitude of response they have to secondary challenges, which results in lower protection as time passes. Nevertheless, this is the first study to demonstrate LPS-induced bacterial protection as far as 28 days. It would be interesting to look at later time points to see how much longer the protection may last, or it may eventually return to its original state following an acute dose of LPS.

Based on the current observations, there are many factors that could contribute to protection following a secondary bacterial challenge. Many studies in the field of TII have found metabolic intermediates to directly play a role in the downstream epigenetic rewiring of pro-inflammatory genes, making them more accessible upon secondary stimulation by either homologous or heterologous pathogens (Netea et al., 2020). It is possible that epigenetic rewiring occurred following LPS exposure, and it would explain why LPS-exposed AMs acquired higher levels of CD11b than their naïve counterparts (Figures 9G and 9I). Since CD11b, together with CD18,

plays a crucial role in leukocyte extravasation and phagocytosis, it would make sense for LPS exposure to protect against subsequent bacterial infections, as evidenced in other studies as well (Seeley et al., 2016). It is also likely for other cell subsets to be involved in the protection. For instance, there was a significantly higher infiltration of neutrophils in LPS-exposed mice compared to naïve mice (Figures 9C and 9D). Neutrophilic responses may help control bacterial burden through the release of extracellular traps and granules. While we did not look at earlier time points, early control of bacterial burden may avoid excessive tissue damage reflected by weight, as seen in our results (Figure 8B). There is lower TNF- α production in the BAL six hours post-infection (Figure 9H). It could be the case that TNF- α production is restricted following LPS exposure in order to prevent excess inflammation and damage to the lungs or that less TNF- α production results due to better control of bacterial infection. However, given that neutrophil counts are higher in the BAL of mice exposed to LPS (Figures 9C and 9D), it is possible that peak TNF- α production may have happened earlier in LPS-exposed mice. In ALI, the crosstalk between AMs and the lung epithelium is indispensable for wound healing (Cheng et al., 2020). Unfortunately, AM-produced molecules for tissue repair are rarely defined, and there is little information on the crosstalk between AMs and the lung epithelium. Additional investigations into the lung epithelium and their role in training will be important in furthering our understanding of this phenomenon.

Based on the findings, BF AM numbers decrease significantly ($\sim 2.5 \times 10^5$ cells) 3 days following LPS exposure, while TransAMs only increase modestly ($\sim 4 \times 10^3$ cells). Likewise, following *S. pneumoniae* infection, BF AM number decreased in half ($\sim 1.5 \times 10^5$ cells) while TransAMs increased by $\sim 1.5 \times 10^3$ cells. It is clear that not all loss from BF AMs is due to their acquisition of CD11b and becoming TransAMs as their pyroptosis or apoptosis following inflammatory insults could also have played a role (Wu et al., 2015). However, the phenotyping and PKH data indicate that BF AM recovered their numbers and are mostly of resident origin on day 14. In addition to that, LPS-exposed BF AMs gain higher CD11b expression following bacterial infection. Taken altogether, this indicates self-renewal of AMs, which may carry pro-inflammatory epigenetic marks to replicated cells. In a study done by Mould et al., 2017, the authors found that 20% of BF AMs incorporated BrdU at peak inflammation (day 3). In addition, they observed high DNA replication in resident macrophages rather than in recruited macrophages, which is in line with the idea that recruited macrophages die off as inflammation resolves (Mould et al., 2017).

There are several caveats to this study. First and foremost, *in vivo* labelling of BF AMs using the PKH26 dye is not sufficient to determine the origin of airway macrophages. We cannot rule out the possibility of recruited monocytes phagocytosing pyroptotic BF AMs and subsequently expressing PKH, which makes them seem like they are of resident origin. In addition, many of the *ex vivo* studies, such as ones that assessed cytokine production and metabolic activity, do

not distinguish between separate airway macrophage populations, and thus, it is still not possible to identify the functional differences between BF AMs, TransAMs, and IMs. Further research, such as transcriptomic profiling or the use of bone marrow chimeras, is needed to separate populations and elucidate their respective roles in the context of LPS-induced ALI.

5. CONCLUSIONS AND FUTURE DIRECTIONS

The major findings from this project are summarized in Figure 10. In brief, following a single respiratory mucosal exposure to LPS, a significant portion of AMs are depleted following LPS exposure. In response to this, neutrophils, MDMs, and IMs are recruited to the airways. On day 14, neutrophil responses have subsided, and the airway macrophage pool is replenished once again, consisting of mainly BF AMs, some IMs, and a few TransAMs. At this time point, there is decreased bacterial burden in the lung following sublethal *S. pneumoniae* infection, possibly due to higher acquisition of CD11b. There is also differential cytokine production following *in vivo* and *ex vivo* secondary stimulation. At day 28, most TransAMs lose their CD11b expression and become akin to BF AMs, although there is protection against bacterial infections seen at this time point.

Although we gained further insight into LPS and its phenotypic and functional effects on the lung, the observations from this project have raised many more questions. For instance, the association between epigenetics and faster acquisition of CD11b should be addressed in future studies. Furthermore, the role of CD11b

in phagocytosis should be confirmed by infecting LPS-exposed mice with labeled *S. pneumoniae* and subsequently examining TransAMs using microscopy or flow cytometry. As mentioned before, the mechanism behind the seen protection is not clear yet. Adoptive transfer of airway macrophages or neutrophil depletion studies can be done to assess the role of individual cell subsets. It may also be worthwhile to dive deeper into pathology and crosstalk with the lung epithelium. In addition to that, phenotyping cell subsets at multiple time points following *S. pneumoniae* may be helpful to confirm if LPS-exposed mice recruit neutrophils and acquire CD11b expression faster than naïve mice. One of the caveats of this project is that airway macrophage subsets could not be separated from each other. Bone marrow chimeras can be used to separate resident and recruited macrophages. In addition to that, gene expression can be examined to determine the ontogeny of airway macrophages and whether there is any difference in their functionality (i.e., phagocytosis and metabolism genes). Future studies should also look at protection beyond 28 days and whether an acute dose of LPS truly has no effect on innate immune memory in the circulation.

A lot of the existing work done on LPS in the context of TII is through systemic administration or in *in vivo* settings. To our knowledge, this is the first project that reports long-lasting training effects induced by local mucosal exposure to LPS in the lung. The results will help us close knowledge gaps in the field of TII, especially concerning the effect of respiratory mucosal LPS exposure on the induction of innate immune memory and its relative contribution to heterologous protection in

the lungs. It will also help us explore the kinetics and ontogeny of airway populations following local mucosal exposure to inflammatory agonists. If proven to be effective, LPS may be used as an adjuvant in developing novel vaccine strategies to confer not only specific protection against one pathogen but also provide cross-protective efficacy against a range of infections. Likewise, this study would also highlight the advantages of using LPS therapeutically as immunomodulatory agents against respiratory infections.

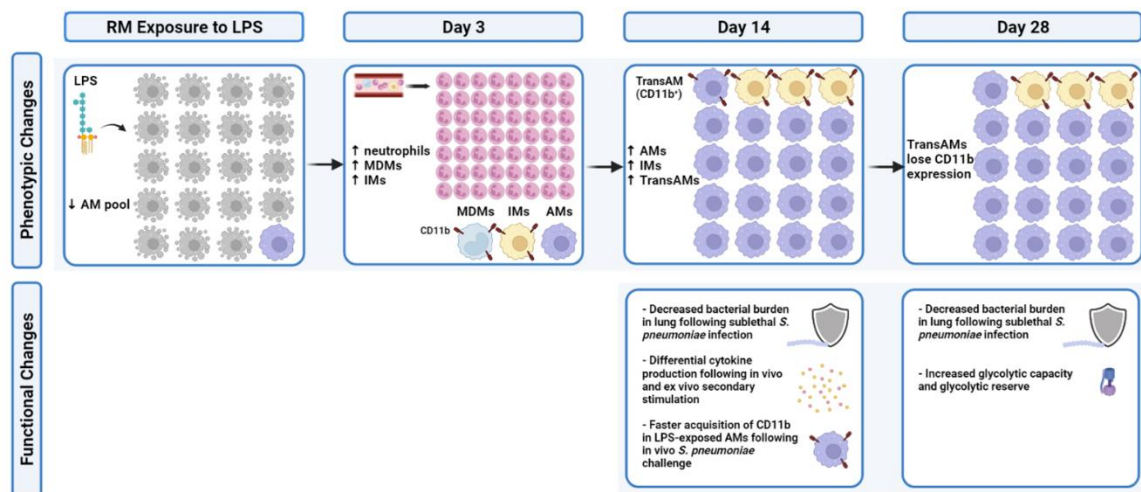


Figure 10. Illustration of main findings from this project

Following local mucosal exposure to LPS, a significant portion of AMs are depleted on day 3. Neutrophils, MDMs, IMs, and TransAMs are seen in the BAL at this time point. On day 14, the airway macrophage pool returns to baseline numbers, and few AMs still express high CD11b expression. At this time point, airway macrophages produce differential cytokine production following secondary stimulation, and also decrease bacterial burden of *S. pneumoniae* in the lungs, possibly due to faster acquisition of CD11b. On day 28, most TransAMs have lost CD11b expression, yet airway macrophages at this time point still display increased glycolytic capacity and reserve, as well as protection against *S. pneumoniae* in the lung.

6. REFERENCES

- Afkhami S, D'Agostino MR, Zhang A, Stacey HD, Marzok A, Kang A, Singh R, Bavananthasivam J, Ye G, Luo X, Wang F, Ang JC, Zganiacz A, Sankar U, Kazhdan N, Koenig JFE, Phelps A, Gameiro SF, Tang S, Jordana M, Wan Y, Mossman KL, Jeyanathan M, Gillgrass A, Medina MFC, Smaill F, Lichty BD, Miller MS, Xing Z. Respiratory mucosal delivery of next-generation COVID-19 vaccine provides robust protection against both ancestral and variant strains of SARS-CoV-2. *Cell*. 2022 Mar 3;185(5):896-915.e19.
- Arts RJ, Novakovic B, Ter Horst R, Carvalho A, Bekkering S, Lachmandas E, Rodrigues F, Silvestre R, Cheng SC, Wang SY, Habibi E, Gonçalves LG, Mesquita I, Cunha C, van Laarhoven A, van de Veerdonk FL, Williams DL, van der Meer JW, Logie C, O'Neill LA, Dinarello CA, Riksen NP, van Crevel R, Clish C, Notebaart RA, Joosten LA, Stunnenberg HG, Xavier RJ, Netea MG. Glutaminolysis and Fumarate Accumulation Integrate Immunometabolic and Epigenetic Programs in Trained Immunity. *Cell Metab*. 2016;24(6):807-819.
- Bekkering S, Arts RJW, Novakovic B, Kourtzelis I, van der Heijden CDCC, Li Y, Popa CD, Ter Horst R, van Tuijl J, Netea-Maier RT, van de Veerdonk FL, Chavakis T, Joosten LAB, van der Meer JWM, Stunnenberg H, Riksen NP, Netea MG. Metabolic Induction of Trained Immunity through the Mevalonate Pathway. *Cell*. 2018;172(1-2):135-146.e9.

- Bekkering S, Quintin J, Joosten LA, van der Meer JW, Netea MG, Riksen NP. Oxidized low-density lipoprotein induces long-term proinflammatory cytokine production and foam cell formation via epigenetic reprogramming of monocytes. *Arterioscler Thromb Vasc Biol.* 2014;34(8):1731-8.
- Bistoni F, Vecchiarelli A, Cenci E, Puccetti P, Marconi P, Cassone A. Evidence for macrophage-mediated protection against lethal *Candida albicans* infection. *Infect Immun.* 1986;51(2):668-74.
- Bistoni F, Verducci G, Perito S, Vecchiarelli A, Puccetti P, Marconi P, Cassone A. Immunomodulation by a low-virulence, agerminative variant of *Candida albicans*. Further evidence for macrophage activation as one of the effector mechanisms of nonspecific anti-infectious protection. *J Med Vet Mycol.* 1988;26(5):285-99.
- Brooks LRK, Mias GI. *Streptococcus pneumoniae*'s virulence and host immunity: aging, diagnostics, and prevention. *Front Immunol.* 2018;9:1366.
- Camilli G, Tabouret G, Quintin J. The complexity of fungal β -glucan in health and disease: effects on the mononuclear phagocyte system. *Front Immunol.* 2018;9:673.
- Cheng P, Li S, Chen H. Macrophages in Lung Injury, Repair, and Fibrosis. *Cells.* 2021; 10(2):436.

Crişan TO, Cleophas MC, Oosting M, Lemmers H, Toenhake-Dijkstra H, Netea MG, Jansen TL, Joosten LA. Soluble uric acid primes TLR-induced proinflammatory cytokine production by human primary cells via inhibition of IL-1Ra. *Ann Rheum Dis*. 2016;75(4):755-62.

D'Agostino MR, Lai R, Afkhami S, Khera A, Yao Y, Vaseghi-Shanjani M, Zganiacz A, Jeyanathan M, Xing Z. Airway Macrophages Mediate Mucosal Vaccine-Induced Trained Innate Immunity against Mycobacterium tuberculosis in Early Stages of Infection. *J Immunol*. 2020;205(10):2750-2762.

Dockrell DH, Marriott HM, Prince LP, et al. Alveolar macrophage apoptosis contributes to pneumococcal clearance in a resolving model of pulmonary infection. *J Immunol* 2003;171:5380-5388.

Dominguez-Andres J, Netea MG. Long-term reprogramming of the innate immune system. *J Leukoc Biol*. 2019;105:329-338.

Domínguez-Andrés J, Novakovic B, Li Y, Scicluna BP, Gresnigt MS, Arts RJW, Oosting M, Moorlag SJCFM, Groh LA, Zwaag J, Koch RM, Ter Horst R, Joosten LAB, Wijmenga C, Michelucci A, van der Poll T, Kox M, Pickkers P, Kumar V, Stunnenberg H, Netea MG. The itaconate pathway is a central regulatory node linking innate immune tolerance and trained immunity. *Cell Metab*. 2019;29:211-220.

Durrant WE, Dong X. Systemic acquired resistance. *Annu. Rev. Phytopathol*. 2004;42:185-209.

Foster SL, Hargreaves DC, Medzhitov R. Gene-specific control of inflammation by TLR-induced chromatin modifications. *Nature*. 2007 Jun 21;447(7147):972-8.

G.P. Youmans, A.S. Youmans. Nonspecific factors in resistance of mice to experimental tuberculosis. *J. Bacteriol.*, 90 (1965), pp. 1675-1681

Gardiner, C.M., Mills, K.H.G. The cells that mediate innate immune memory and their functional significance in inflammatory and infectious diseases. *Semin Immunol*. 2016 Aug;28(4):343-50.

Garly ML, Martins CL, Balé C, Baldé MA, Hedegaard KL, Gustafson P, Lisse IM, Whittle HC, Aaby P. BCG scar and positive tuberculin reaction associated with reduced child mortality in West Africa. A non-specific beneficial effect of BCG? *Vaccine*. 2003;21(21-22):2782-90.

Gibbins SL, Goyal R, Desch AN, Leach SM, Prabagar M, Atif SM, Bratton DL, Janssen W, Jakubzick CV. Transcriptome analysis highlights the conserved difference between embryonic and postnatal-derived alveolar macrophages. *Blood*. 2015;126:1357–1366.

Goodridge HS, Wolf AJ, Underhill DM. Beta-glucan recognition by the innate immune system. *Immunol Rev*. 2009;230(1):38-50.

Gourbal B, Pinaud S, Beckers GJM, Van Der Meer JWM, Conrath U, Netea MG. Innate immune memory: an evolutionary perspective. *Immunol Rev*. 2018;283:21-40.

Guilliams M, De Kleer I, Henri S, Post S, Vanhoutte L, De Prijck S, Deswarte K, Malissen B, Hammad H, Lambrecht BN. Alveolar macrophages develop from fetal monocytes that differentiate into long-lived cells in the first week of life via GM-CSF. *J. Exp. Med.* 2013;210(10):1977-92.

Guilliams, M, Svedberg, FR. Does tissue imprinting restrict macrophage plasticity? *Nat Immunol* 2021;22,118-127.

Hashimoto D, Chow A, Noizat C, Teo P, Beasley MB, Leboeuf M, Becker CD, See P, Price J, Lucas D, Greter M, Mortha A, Boyer SW, Forsberg EC, Tanaka M, van Rooijen N, García-Sastre A, Stanley ER, Ginhoux F, Frenette PS, Merad M. Tissue-resident macrophages self-maintain locally throughout adult life with minimal contribution from circulating monocytes. *Immunity.* 2013;38:792–804.

Hildemann WH, Johnson IS, Jokiel PL. Immunocompetence in the lowest metazoan phylum: transplantation immunity in sponges. *Science.* 1979;204:420-422.

Hildemann WH, Raison RL, Cheung G, Hull CJ, Akaka L, Okamoto J. Immunological specificity and memory in a scleractinian coral. *Nature.* 1977;270:219-223.

Hussell T, Bell TJ. Alveolar macrophages: plasticity in a tissue-specific context. *Nature Rev Immunol.* 2014;14,81-93.

Joosten LAB, Crişan TO, Bjornstad P, Johnson RJ. Asymptomatic hyperuricaemia: a silent activator of the innate immune system. *Nat Rev Rheumatol*. 2020;16(2):75-86.

Kalafati L, Kourtzelis I, Schulte-Schrepping J, Li X, Hatzioannou A, Grinenko T, Hagag E, Sinha A, Has C, Dietz S, de Jesus Domingues AM, Nati M, Sormendi S, Neuwirth A, Chatzigeorgiou A, Ziogas A, Lesche M, Dahl A, Henry I, Subramanian P, Wielockx B, Murray P, Mirtschink P, Chung KJ, Schultze JL, Netea MG, Hajishengallis G, Verginis P, Mitroulis I, Chavakis T. Innate Immune Training of Granulopoiesis Promotes Anti-tumor Activity. *Cell*. 2020;183(3):771-785.e12.

Kaufmann E, Sanz J, Dunn JL, Khan N, Mendonça LE, Pacis A, Tzelepis F, Pernet E, Dumaine A, Grenier JC, Mailhot-Léonard F, Ahmed E, Belle J, Besla R, Mazer B, King IL, Nijnik A, Robbins CS, Barreiro LB, Divangahi M. BCG Educates Hematopoietic Stem Cells to Generate Protective Innate Immunity against Tuberculosis. *Cell*. 2018;172(1-2):176-190.e19.

Knapp S, Leemans JC, Florquin S, Branger J, Maris NA, Pater J, van Rooijen N, van der Poll T. Alveolar macrophages have a protective anti-inflammatory role during murine pneumococcal pneumoniae. *Am J Respir Crit Care Med* 2003;167:171-179.

Kopf M, Schneider C, Nobs SP. The development and function of lung-resident macrophages and dendritic cells. *Nat. Immunol*. 2015;16(1):36-44.

Krahenbuhl, JL, Sharm SD, Ferraresi, RW & Remington, JS. Effects of muramyl dipeptide treatment on resistance to infection with *Toxoplasma gondii* in mice. *Infect. Immun.* 1981;31:716-722.

Landsman L, and Jung S. Lung macrophages serve as obligatory intermediate between blood monocytes and alveolar macrophages. *J. Immunol.* 2007;179:3488–3494.

Lavin Y, Winter D, Blecher-Gonen R, David E, Keren-Shaul H, Merad M, Jung S, Amit I. Tissue-resident macrophage enhancer landscapes are shaped by the local microenvironment. *Cell.* 2014;159:1312–1326.

Machiels B, Dourcy M, Xiao X, Javaux J, Mesnil C, Sabatel C, Desmecht D, Lallemand F, Martinive P, Hammad H, Guilliams M, Dewals B, Vanderplasschen A, Lambrecht BN, Bureau F, Gillet L. A gammaherpesvirus provides protection against allergic asthma by inducing the replacement of resident alveolar macrophages with regulatory monocytes. *Nat Immunol.* 2017 Dec;18(12):1310-1320. doi: 10.1038/ni.3857. Epub 2017 Oct 16. Erratum in: *Nat Immunol.* 2018 Sep;19(9):1035.

Mizobuchi. H, Soma, GI. Low-dose lipopolysaccharide as an immune regulator for homeostasis maintenance in the central nervous system through transformation to neuroprotective microglia. *Neural Regen Res.* 2021 Oct; 16(10):1928-1934.

Moret Y, Siva-Jothy MT. Adaptive innate immunity? Responsive-mode prophylaxis in the mealworm beetle, *Tenebrio molitor*. *Proc. Biol. Sci.* 2003;270:2475-2480.

Mould KJ, Barthel L, Mohning MP, Thomas SM, McCubbrey AL, Danhorn T, Leach SM, Fingerlin TE, O'Connor BP, Reisz JA, D'Alessandro A, Bratton DL, Jakubzick CV, Janssen WJ. Cell Origin Dictates Programming of Resident versus Recruited Macrophages during Acute Lung Injury. *Am J Respir Cell Mol Biol.* 2017 Sep;57(3):294-306.

Muñoz N, Van Maele L, Marques JM, Rial A, Sirard JC, Chabalgoity JA. Mucosal administration of flagellin protects mice from *Streptococcus pneumoniae* lung infection. *Infect. Immun.* 2010 Oct;78(10):4226–33.

Murphy KM, Weaver C, Mowat A, Berg L, Chaplin D, Janeway CA, Travers P, Walport M. *Janeway's immunobiology* (9th ed.) 2017. New York London Gs, Garland Science, Taylor & Francis Group.

Natarajan S, Kim J, Remick DG. Chronic pulmonary LPS tolerance induces selective immunosuppression while maintaining the neutrophilic response. *Shock.* 2010 Feb;33(2):162-9.

Nelson AL, Roche AM, Gould JM, Chim K, Ratner AJ, Weiser JN. Capsule enhances pneumococcal colonization by limiting mucus-mediated clearance. *Infect Immun* 2007;75(1):83-90.

Netea MG, Domínguez-Andrés J, Barreiro LB, Chavakis T, et al. Defining trained immunity and its role in health and disease. *Nat Rev Immunol.* 2020;20(6):375-388.

Netea MG, Joosten LA, Latz E, Mills KH, Natoli G, Stunnenberg HG, O'Neill LA, Xavier RJ. Trained immunity: a program of innate immune memory in health and disease. *Science.* 2016;352:aaf1098.

Netea MG, van Crevel R. BCG-induced protection: effects on innate immune memory. *Semin Immunol.* 2014;26:512-517.

Pham LN, Dionne MS, Shirasu-Hiza M, Schneider DS. A specific primed immune response in *Drosophila* is dependent on phagocytes. *PLoS Pathog.* 2007;3:e26.

Ribes S, Meister T, Ott M, Redlich S, Janova H, Hanisch UK, Nessler S, Nau R. Intraperitoneal prophylaxis with CpG oligodeoxynucleotides protects neutropenic mice against intracerebral *Escherichia coli* K1 infection. *J. Neuroinflammation* 2014;11,14.

Rieckmann A, Villumsen M, Sørup S, Haugaard LK, Ravn H, Roth A, Baker JL, Benn CS, Aaby P. Vaccinations against smallpox and tuberculosis are associated with better long-term survival: a Danish case-cohort study 1971-2010. *Int. J. Epidemiol.* 2017;46,695-705.

Riksen NP, Netea MG. Immunometabolic control of trained immunity. *Mol Aspects Med.* 2021 Feb;77:100897.

Rodrigues J, Brayner FA, Alves LC, Dixit R, Barillas-Mury C. Hemocyte differentiation mediates innate immune memory in *Anopheles gambiae* mosquitoes. *Science.* 2010;329:1353-1355.

Scott CL, Henri S, Guillemins M. Mononuclear phagocytes of the intestine, the skin, and the lung. *Immunol Rev.* 2014;262(1):9-24.

Seeley, JJ, Ghosh, S. Molecular mechanisms of innate memory and tolerance to LPS. *J. Leuk. Biol.* 2016;101(1):107-119.

Smaill F, Jeyanathan M, Smieja M, Medina MF, Thantrige-Don N, Zganiacz A, Yin C, Heriazon A, Damjanovic D, Puri L, Hamid J, Xie F, Foley R, Bramson J, Gauldie J, Xing Z. A human type 5-adenovirus-based tuberculosis vaccine induces robust T cell responses in humans despite preexisting anti-adenovirus immunity. *Sci. Transl. Med.* 2013;5,205ra134.

Sticher L, Mauch-Mani B, Mettraux JP. Systemic acquired resistance. *Annu. Rev. Phytopathol.* 1997;35:235-270.

Taut K, Winter C, Briles DE, Paton JC, Christman JW, Maus R, Baumann R, Welte T, Maus UA. Macrophage turnover kinetics in the lungs of mice infected with *Streptococcus pneumoniae*. *Am. J. Respir. Cell. Mol. Biol.* 2008;38:105-13.

- Tribouley J, Tribouley-Duret J, Appriou M. Influence du bacille de Calmette et Guérin (BCG) sur la réceptivité de la Souris nude vis-à-vis de *Schistosoma mansoni* [Effect of Bacillus Callmette Guerin (BCG) on the receptivity of nude mice to *Schistosoma mansoni*]. *C R Seances Soc Biol Fil.* 1978;172(5):902-4.
- Uthayakumar D, Paris S, Chapat L, Freyburger L, Poulet H, De Luca K. Non-specific effects of vaccines illustrated through the BCG example: from observations to demonstrations. *Front Immunol.* 2018;9:2869.
- Van de Laar L, Saaelens W, De Prijck S, et al. Yolk Sac Macrophages, Fetal Liver, and Adult Monocytes Can Colonize an Empty Niche and Develop into Functional Tissue-Resident Macrophages. *Immunity.* 2016;44(4):755-68.
- van der Heijden CDCC, Groh L, Keating ST, Kaffa C, Noz MP, Kersten S, van Herwaarden AE, Hoischen A, Joosten LAB, Timmers HJLM, Netea MG, Riksen NP. Catecholamines Induce Trained Immunity in Monocytes In Vitro and In Vivo. *Circ Res.* 2020;127(2):269-283.
- van der Heijden CDCC, Keating ST, Groh L, Joosten LAB, Netea MG, Riksen NP. Aldosterone induces trained immunity: the role of fatty acid synthesis. *Cardiovasc Res.* 2020;116(2):317-328.
- van der Poll T, Opal SM. Pathogenesis, treatment, and prevention of pneumococcal pneumonia. *Lancet.* 2009;374(9700):1543-56.

van 't Wout JW, Poell R, van Furth R. The role of BCG/PPD-activated macrophages in resistance against systemic candidiasis in mice. *Scand J Immunol.* 1992;36(5):713-9

Vecchiarelli A, Cenci E, Puliti M, Blasi E, Puccetti P, Cassone A, Bistoni F. Protective immunity induced by low-virulence *Candida albicans*: cytokine production in the development of the anti-infectious state. *Cell Immunol.* 1989;124(2):334-44.

Wendeln, A.C., Degenhardt, K., Kaurani, L. Innate immune memory in the brain shapes neurological disease hallmarks. *Nature* 2018 Apr; 556(771):332-338.

Willment JA, Marshall AS, Reid DM, Williams DL, Wong SY, Gordon S, Brown GD. The human beta-glucan receptor is widely expressed and functionally equivalent to murine Dectin-1 on primary cells. *Eur J Immunol.* 2005;35(5):1539-47.

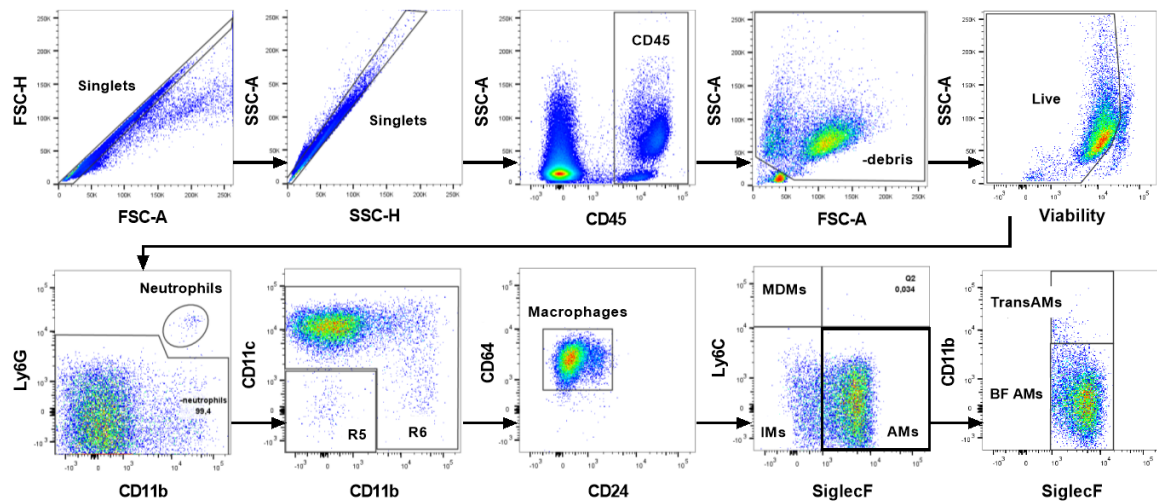
Wu DD, Pan PH, Liu B, Su XL, Zhang LM, Tan HY, Cao Z, Zhou ZR, Li HT, Li HS et al. Inhibition of Alveolar Macrophage Pyroptosis Reduces Lipopolysaccharide-induced Acute Lung Injury in Mice. *Chin. Med. J.* 2015, 128, 2638–2645

Xing Z, Afkhami S, Bavananthasivam J, Fritz DK, D'Agostino MR, Vaseghi-Shanjani M, Yao Y, Jeyanathan M. Innate immune memory of tissue-resident macrophages and trained innate immunity: Re-vamping vaccine concept and strategies. *J. Leuko. Biol.* 2020;108:825-834.

- Yao Y, Jeyanathan M, Haddadi S, Barra NG, Vaseghi-Shanjani M, Damjanovic D, Lai R, Afkhami S, Chen Y, Dvorkin-Gheva A, Robbins CS, Schertzer JD, Xing Z. Induction of Autonomous Memory Alveolar Macrophages Requires T Cell Help and Is Critical to Trained Immunity. *Cell*. 2018;175(6):1634-1650.e17.
- Yin C, Cheng L, Pan J, Chen L, Xue Q, Qin J, Wang S, Du B, Liu M, Zhang Y, Jiang W, Qian M, Ren H. Regulatory role of Gpr84 in the switch of alveolar macrophages from CD11b^{lo} to CD11b^{hi} status during lung injury process. *Mucosal Immunol*. 2020 Nov;13(6):892-907.
- Yona S, Kim KW, Wolf Y, Mildner A, Varol D, Breker M, Strauss-Ayali D, Viukov S, Guilliams M, Misharin A, Hume DA, Perlman H, Malissen B, Zelzer E, Jung S. Fate mapping reveals origins and dynamics of monocytes and tissue macrophages under homeostasis. *Immunity*. 2013;38(1):79-91.
- Zhang B, Chassaing B, Shi Z, Uchiyama R, Zhang Z, Denning TL, Crawford SE, Pruijssers AJ, Iskarpatyoti JA, Estes MK, Dermody TS, Ouyang W, Williams IR, Vijay-Kumar M, Gewirtz AT. Viral infection. Prevention and cure of rotavirus infection via TLR5/NLRC4-mediated production of IL-22 and IL-18. *Science* 2014;346, 861–865.

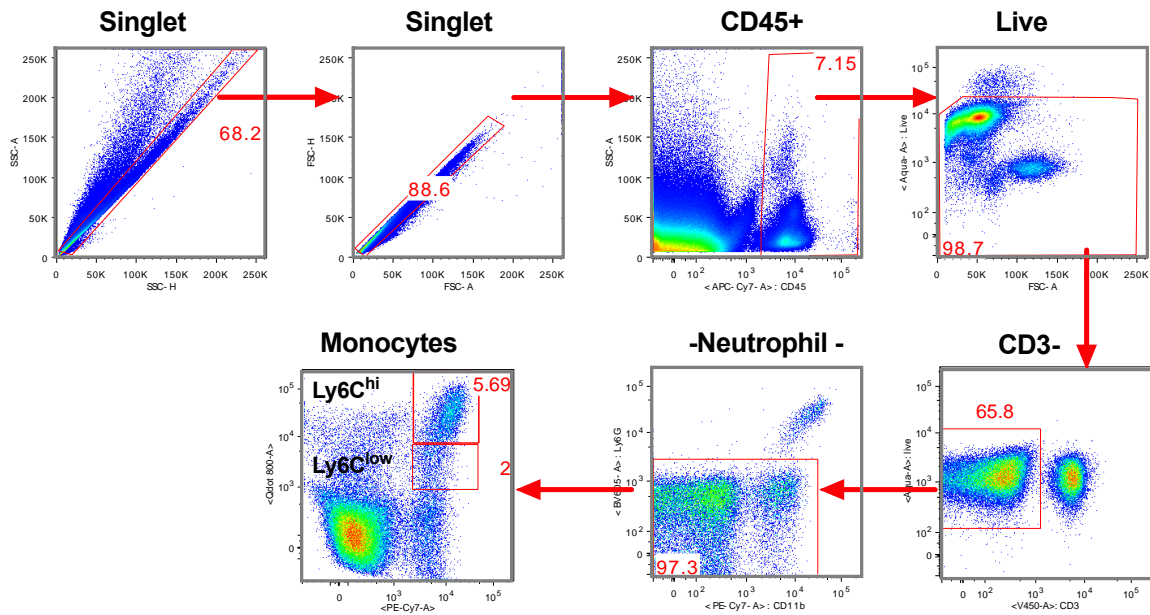
7. SUPPLEMENTAL FIGURES

Supplemental Figure 1. Comprehensive flow cytometry gating strategy for airway macrophages in BAL.



Gating strategy to distinguish between airway macrophage subsets (i.e., monocyte-derived macrophages (MDMs), interstitial macrophages (IMs), transitioning AMs (TransAMs), and bona fide AMs (BF AMs)) in the airway lumen (BAL) based on a comprehensive flow cytometry immunostaining panel. The example shown here was on BAL isolated 14 days post-LPS exposure in order to display the TransAM population.

Supplemental Figure 2. Comprehensive flow cytometry gating strategy for circulating monocytes in blood.



Gating strategy to distinguish between circulating monocytes subsets (i.e., Ly6C^{hi} and Ly6C^{lo} monocytes) in blood based on a comprehensive flow cytometry immunostaining panel. The example shown here was on blood isolated 14 days post-LPS exposure and WCL stimulation.